

**SHEAR STRENGTH AND SUCTION PROPERTIES OF NORTH
CYPRUS SANDS**

**A THESIS SUBMITTED TO THE GRADUATE
SCHOOL OF APPLIED SCIENCES
OF
NEAR EAST UNIVERSITY**

**By
ABUBAKAR SANI LAWAL**

**In Partial Fulfillment of the Requirements for
the Degree of Master of Science
in
Civil Engineering**

NICOSIA, 2018.

ABUBAKAR SANI LAWAL

**SHEAR STRENGTH AND SUCTION PROPERTIES OF NORTH CYPRUS
SANDS NEU**

2018

**SHEAR STRENGTH AND SUCTION PROPERTIES OF
NORTH CYPRUS SANDS**

**A THESIS SUBMITTED TO THE GRADUATE
SCHOOL OF APPLIED SCIENCES
OF
NEAR EAST UNIVERSITY**

**By
ABUBAKAR SANI LAWAL**

**In Partial Fulfillment of the Requirements for
the Degree of Master of Science
in
Civil Engineering**

NICOSIA, 2018.

**Abubakar Sani Lawal: SHEAR STRENGTH AND SUCTION PROPERTIES OF
NORTH CYPRUS SANDS**

**Approval of Director of Graduate School of
Applied Sciences**

Prof. Dr. Nadire Çavuş

**We certify that, this thesis is satisfactory for the award of the degree of Master of
Science
In Civil Engineering**

Examining Committee in Charge:

Prof. Dr. Hüseyin Gökçekuş

Chairman, Department of Civil
Engineering, NEU

Assoc. Prof. Dr. Huriye Bilsel

Department of Civil Engineering, CIU

Dr. Anoosheh Iravanian

Supervisor, Department of Civil
Engineering, NEU

I hereby declare that all information in this document has been obtained and presented in accordance with academic rules and ethical conduct. I also declare that, as required by these rules and conduct, I have fully cited and referenced all material and results that are not original to this work.

Name, Last name: Abubakar Sani Lawal

Signature:

Date:

ACKNOWLEDGEMENTS

All thanks and praise are to Allah The One and Only, and peace and blessings be to Prophet Muhammad. It is with Allah's glory that I was able to complete this thesis.

I will never feel blessed enough to have such incredible parents, my father Alhaji Sani Lawal and my mother Hajiya Mariya Garba. You gave me unwithheld love and care together with needed guidance on how to always become a better person. It is with your guidance that I challenged myself to complete this thesis. I love you mom and dad.

Having such an excellent supervisor as Dr. Anoosheh Iravanian was what made this thesis possible. You showed me amazing support and gave me the push I needed whenever I got held back. Such effort shall not be forgotten. Thank you very much.

My siblings are the best. They've always been there for me my whole life. Basheer, Aisha and Ismail, love you guys. I've been blessed with many friends through my journey who made it easier for me to endure the hard work during periods of studying and to enjoy the fun in between those periods. I cannot mention you all, but you know yourselves.

I would like to also extend my words of gratitude to Dr. Mehmet Necdet for helping me obtain the sand samples from their sources, and to Assoc. Prof. Dr. Huriye Bilsel for her help in providing me with the tubes for the experiments. Thank you, Mustafa Turk, laboratory technician at Near East University, for your assistance. I would like to also thank the civil engineering department of Eastern Mediterranean University for their cooperation and assistance by granting us permission to use the SoilVision software program available in their laboratory.

To my Mom and Dad

ABSTRACT

Suction properties are influential on the shear strength of unsaturated soils. North Cyprus has different types of sands that could be investigated from the suction and shear strength characteristics point of view. Natural sea sand, crushed limestone and yellow sand of North Cyprus are the types of sand that are experimentally studied in this thesis.

Shear strength of a soil provides resistance against stress exerted along a horizontal plane. The shear strength of any given soil is affected by its suction capability. Shear strength test can help obtain the values of parameters like angle of friction and cohesion of the tested soil. Suction means the capacity of soil to absorb water. The three components of suction are matric suction, osmotic suction and total suction.

The Tube Suction Test (TST) was used to calculate the matric suction while shear strength test was conducted using Direct Shear Test (DST). The samples consist of natural sea sand from Gaziveren (GAZ), yellow sand from Serhatköy and two crushed limestone sands from Gürdal (GÜR) and Roads Department Quarry (RDQ).

SoilVison software is used to fit 'Fredlund and Xing' and 'van Genuchten (1980)' formulas to predict the soil water characteristics curve, SWCC, for the sand samples. Results indicated that the more the matric suction, the less moisture content the sand contained. Angle of friction seemed to decrease as the moisture content increased. The shear strength of each sample increased with increasing matric suction.

Keywords: Sand; shear strength; suction; SWCC; tube suction test

ÖZET

Emme basıncı, yarı doymun zeminlerde kayma mukavemeti üzerinde etkili bir faktördür. Kuzey Kıbrıs bölgesindeki kum alanlar, emme basıncı ve kayma mukavemeti açısından farklılık gösterdiğinden dolayı, bahsi geçen faktörlerin araştırılması gerekmektedir. Bu çalışma, doğal deniz kumu, kırık kireç taşı ve sarı kum üzerinde araştırmaları içermektedir.

Zemindeki kayma mukavemeti, yatay düzlemde direnç oluşumuna sebep olur. Herhangi bir zeminin kayma mukavemeti, zeminin emme kapasitesi ile orantılıdır. Kayma mukavemeti deneyleri sayesinde, sürtünme açısı, kohezyon katsayısı gibi parametreler elde edilebilir. Emme; zeminin suyu özümseme kapasitesidir Emme çeşitleri; matrik emme, ozmotik emme ve toplam emme olarak sıralanabilir.

Bu çalışma kapsamında; matrik emme için Emme Tüpü Testi ve kayma mukavemeti ölçümü için kesme kutusu deneyi uygulanmıştır. Bahsi geçen testler; Gaziveren bölgesine ait doğal deniz kumu, Serhatköy bölgesine ait sarı kum, Gürdal ve Karayolları Dairesi'ne aid taş ocaklarında, kırık kireç taşı örnekleri üzerinde uygulanmıştır.

Örneklerin zemin su karakteristik eğrisi, SWCC, değerlerini öngörmek için 'Fredlund ve Xing' ve 'Van Genuchten (1980)' denklemleri uygulanmıştır. SoilVision isimli bilgisayar yazılımında elde edilen sonuçlara göre; matrik emme değeri yüksek olan verilere ait örneklerin su muhtevası düştüğü ortaya çıkmıştır. Buna ek olarak sürtünme açısının yükseldikçe su muhtevasının düştüğü gözlenmiştir. Kayma mukavemeti ise; matrik emme ile doğru orantılı davranış göstermiştir.

Anahtar kelimeler: Kum; kayma mukavemeti; emme basıncı; SWCC; Emme Tüpü Testi

TABLE OF CONTENTS

ACKNOWLEDGEMENTS	i
ABSTRACT	iii
ÖZET	iv
TABLE OF CONTENTS	v
LIST OF TABLES	vii
LIST OF FIGURES	viii
LIST OF SYMBOLS AND ABBREVIATIONS	xi
CHAPTER 1: INTRODUCTION	
1.1 Background.....	1
1.2 Importance and Objectives	2
1.3 Scope of Research.....	3
1.4 Previous Research.....	3
1.5 Thesis format	4
CHAPTER 2: LITERATURE REVIEW	
2.1 Sand	6
2.1.1 Natural Sand	6
2.1.2 Sandstone.....	9
2.1.3 Crushed Sand	10
2.2 Shear Strength.....	11
2.2.1 Mohr’s Circle.....	14
2.2.2 Normal and Shear Stresses	15
2.2.3 Dilation	16

2.3 Suction In Unsaturated Soil	18
2.3.1 Suction Measurement Methods	19
2.4 Soil-Water Characteristics Curve (SWCC)	29
 CHAPTER 3: METHODOLOGY	
3.1 Samples.....	33
3.2 Tube Suction Test (TST)	38
3.3 Direct Shear Test (DST)	39
 CHAPTER 4: RESULTS AND DISCUSSIONS	
4.1 Samples.....	41
4.2 Direct Shear Test (DST)	42
4.3 Soil-Water Characteristics Curve (SWCC)	48
4.4 Matric Suction And Shear Strength.....	55
 CHAPTER 5: CONCLUSION AND RECOMMENDATIONS	
5.1 Conclusion	59
5.2 Recommendations.....	59
 REFERENCES.....	 60

LIST OF TABLES

Table 2.1: Different classifications of sand by various agricultural and Engineering organisations	6
Table 2.2: Common values of friction angle of silts and sands.....	15
Table 2.3: The summary of different methods and techniques for measuring suction.....	28
Table 3.1: Sieve number and sizes used in the sieve analysis of the soil samples	37
Table 4.1: Physical properties of soil samples	42
Table 4.2: Comparison of shear strength parameter values of all four samples under the three water contents, 0%, 5% and 10%.	47
Table 4.3: Comparison of RWC and AEV of both Fredlund and Xing (1994) and van Genuchten (1980) fit for GAZ.....	51
Table 4.4: Comparison of RWC and AEV of both Fredlund and Xing (1994) and van Genuchten (1980) fit for GÜR.....	52
Table 4.5: Comparison of RWC and AEV of both Fredlund and Xing (1994) and van Genuchten (1980) fit for SER.....	53
Table 4.6: Comparison of RWC and AEV of both Fredlund and Xing (1994) and van Genuchten (1980) fit for RDQ.....	54
Table 4.7: Comparison of shear strength and matric suction of all samples under three normal stresses.....	59
Table 4.8: Comparison of graph trends of matric suction and shear strength comparison for all four samples under the three normal stresses, 27.8, 55.6 and 83.3 kPa	59

LIST OF FIGURES

Figure 2.1: Stages of sand particle formation.....	8
Figure 2.2: Shapes of sand particle.....	9
Figure 2.3: Blocks of carved sandstone at Serhatköy, North Cyprus.....	10
Figure 2.4: Diagram of direct shear test arrangement	13
Figure 2.5: The Mohr-Coulomb failure criterion	14
Figure 2.6: The graph soil displacement during shearing	17
Figure 2.7: Direct shear test results in loose, medium, and dense sands.....	17
Figure 2.8: TST Setup with electric probes.....	20
Figure 2.9: Diagram illustrating capillary rise.....	21
Figure 2.10: A full setup of a TDR test	24
Figure 2.11: A diagram of non-contact filter paper technique	25
Figure 2.12: An example of SWCC	29
Figure 3.1: A sample of GAZ used in the laboratory	33
Figure 3.2: Huge deposit of GAZ sand.....	34
Figure 3.3: Sample of GÜR (a) and RDQ (b) used in the laboratory.....	34
Figure 3.4: The parent rock and crushed sand deposit for RDQ (a) and GÜR (b).....	35
Figure 3.5: A sample of SER used in the laboratory	35
Figure 3.6: Yellow sand deposit from sandstone mine (SER)	36
Figure 3.7: The setup for specific gravity in the laboratory	37

Figure 3.8: Shaking able used for relative density test.....	38
Figure 3.9: The soil tube place in a bucket of water after loading samples. Retrieval holes have been covered with tapes to prevent sample loss.....	39
Figure 3.10: DST setup used in the laboratory.....	40
Figure 4.1: Particle size distribution curve of the four samples	41
Figure 4.2: Normal Stress vs Shear Stress for GAZ.....	43
Figure 4.3: Normal Stress vs Shear Stress for GÜR	44
Figure 4.4: Normal Stress vs Shear Stress for SER.....	45
Figure 4.5: Normal Stress vs Shear Stress for RDQ.....	46
Figure 4.6: Comparison between cohesion and angle of friction for GAZ and RDQ samples	47
Figure 4.7: Comparison between cohesion and angle of friction for SER and GÜR samples	48
Figure 4.8: The SWCC for drying suction procedure comparing the resulting water contents of all four samples	49
Figure 4.9: The SWCC for wetting suction procedure comparing the resulting water contents of all four samples.	49
Figure 4.10: Fredlund and Xing (1994) and van Genuchten (1980) fits for both drying and wetting processes for GAZ.....	51
Figure 4.11: Fredlund and Xing (1994) and van Genuchten (1980) fits for both drying and wetting processes for GÜR.....	52
Figure 4.12: Fredlund and Xing (1994) and van Genuchten (1980) fits for both drying and wetting processes for SER.....	53

Figure 4.13: Fredlund and Xing (1994) and van Genuchten (1980) fits for both drying and wetting processes for RDQ.....	54
Figure 4.14: Matric Suction vs Shear Strength for GAZ under 19.2 kPa, 57.7 kPa and 96.2 kPa normal stresses	55
Figure 4.15: Matric Suction vs Shear Strength for GÜR under 19.2 kPa, 57.7 kPa and 96.2 kPa normal stresses	56
Figure 4.16: Matric Suction vs Shear Strength for RDQ under 19.2 kPa, 57.7 kPa and 96.2 kPa normal stresses	58

LIST OF SYMBOLS AND ABBREVIATIONS

ASTM:	American Society for Testing and Materials
BS:	British Standard
c:	Effective cohesion
DST:	Direct Shear Test
GAZ:	Gaziveren
GÜR:	Gürdal
P_{at}:	Atmospheric pressure
RDQ:	Roads Department Quarry
SER:	Serhatköy
SWCC:	Soil-Water Characteristics Curve
u:	Matric suction
u_a:	Air-entry suction of soil
USCS:	Unified Soil Classification System
u_w:	Pore water pressure of soil
WRC:	Water Retention Curve
σ:	Normal stress
τ:	Shear strength
φ:	Effective friction angle

CHAPTER 1

INTRODUCTION

1.1 Background of Studies

Sand is a crucial material in several uses in civil engineering. Sand is generally known to have particles between 0.075 and 4.75 mm in diameter, though classification differs from different organisations (Das, 2008). Sand can be formed naturally through different processes from weathering, erosion and transportation. It can also be formed by crushing in mines and quarries. Natural sand generally contains particles created from quartz and feldspar. Grains formed from other minerals such as calcite, mica and fragments of limestone, slate and basalt can also be found (Das, 2008). Crushed sand can be found abundantly in limestone quarries and utilising it could decrease cost of concrete while helping with disposal cost and environmental pollution. The availability of crushed sand as by product from quarries has brought about a shift from natural sand (Menadi et al., 2009).

The availability of both natural and crushed sands in North Cyprus means it is important to examine their physical properties for comparison and further research. There are a variety of natural sands on the island such as river sand, sea sand from beaches and sea sand deposited long time ago. Crushed sands found include crushed limestone sand and yellow sand. Locations of the sources of the sands used in this research are shown in Figure 1.1

The shear strength of a soil is basically its resistance to failure along a plane if exposed to stress. It consists of different parameters such as angle of friction, normal stress, and cohesion. The Mohr-Coulumb envelope is used to determine the angle of friction using shear stress and normal stress data obtained from the laboratory tests (Adunoye, 2014). Introduction of different particle size into a sample causes a change in its shear strength parameters (Fu et al., 2015).

Suction is simply the ability of soil to absorb water. It can be calculated in three different forms; matric suction, osmotic suction and total suction. Total suction is also the sum of matric suction and osmotic suction (Çokça & Tilgen, 2010). The graph that compares suction with water content is referred to as Soil-Water Characteristics Curve (SWCC). SWCC curves can be predicted and modelled using formulas made by soil experts such as the Fredlund and Xing (1994) fit and van Genuchten (1980) fit. The SoilVision software has a feature that can fit such equations with suction data obtained from the laboratory. Shear strength is affected by change in water content caused by matric suction (Çokça & Tilgen, 2010).



Figure 1.1: Locations of sample origins around North Cyprus

1.2 Importance and Objectives

Suction properties of sand can well affect its shear strength due to change in water content resulting from absorption ability of the sand. Previous researches in Turkey and other countries around the world have investigated the relationship between suction and shear

strength of different types of soil including sand, clay and glacial till. However, there aren't many researches that investigate these properties for sands available in North Cyprus. This research aims to study sands that can be found in North Cyprus and to make comparison between different types of sands. Research on the direct effect of matric suction on the shear strength of these samples can create platform for further researches on the samples but with added gravels or clay as a change.

1.3 Scope of Research

In this study the shear strength and suction of four sand samples were evaluated and compared to assess any relationship. The soil suction is measured using the Tube Suction Test (TST) using special tubes, and the shear strength parameters were calculated using the Direct Shear Test (DST). Suction values were compared with water content and shear strength. The basic soil properties were also evaluated beforehand. The suction test results were used to draw Soil-Water Characteristics Curve (SWCC) using SoilVision software. Fredlund and Xing (1994) and van Genuchten (1980) equations were used to predict the SWCC fit. The research also covers comparison between shear strength and matric suction.

1.4 Previous Researches

In 2004, Farouk et al. did a research to investigate the effects of suction on shear strength performance of unsaturated sand with zero cohesion. The sample is commercially available and is known as PR33. The method used to measure the shear strength of sand was the constant water content triaxial test method, which also determines the matric suction during testing. Results showed that increase in matric suction caused increase in shear strength.

In 1998, Shimada completed a research where the shear strength, as well as the volume change were investigated under effect of matric suction for the unsaturated sand. The sand

was classified as poorly-graded. The method used was the suction-controlled simple shear test. They also conducted a drained test on saturated sample for contrast. There was not much increase in shear strength, and the degree of dilation also got higher as the matric suction was increased.

In 1996, Vanapalli et al. tested a glacial till that was in a compacted state in both saturated and unsaturated form. Consolidated drained direct shear test was used in the research. They also tested samples under varying density value for the samples.

In 2003, Tilgen tested METU Campus clay at different moisture contents dryer and wetter of optimum moisture content of 20.8%. the soil sample was a low plasticity clay (CL). The direct shear test was used to evaluate the shear strength, while filter paper test was used for matric suction evaluation. The shear strength was found to increase as matric suction increased.

In 2009, Çokça and Tilgen tested Ankara clay under same circumstances as Tilgen (2003) and found similar results.

1.5 Thesis format

This report is laid out in chapters that present respective information as follows:

1. **Chapter 1:** This chapter covers introduction to the idea, importance, purpose and basic definitions of the of the project presented in the title. It also states previous researches that have covered a similar topic as this research.
2. **Chapter 2:** Literature Review explains in details the terms and gives definition of topics discussed in the thesis while mentioning important details. Equations, tables and diagrams are included to give extra explanations.

3. **Chapter 3:** Methodology chapter deals with the description of the research procedures starting from sample description and physical properties, to the explanation of test procedures used.
4. **Chapter 4:** Results and discussions chapter covers all analysis of data obtained from the laboratory and from the SoilVision software. Further calculations made from those data are also presented and analysed with comparison between samples.
5. **Chapter 5:** This chapter contains all conclusions and recommendations that can be drawn from the results discussed in chapter 4. It is also the final chapter of the report

CHAPTER 2

LITERATURE REVIEW

2.1 Sand

Sand is generally known to have particles between 0.075 and 4.75 mm in diameter, though classification differs from different organisations (Das, 2008). Table 1 shows the different classifications of sand grain size by various organisations.

Table 2.1: Different classifications of sand by various agricultural and Engineering organisations (Das, 2008)

Name of Organisation	Grain Size (mm)
MIT (Massachusetts Institute of Technology)	0.06 to 2
USDA (US Department of Agriculture)	0.05 to 2
AASHTO (America Association of Highway and Transport Officials)	0.075 to 2
USCS (Unified Soil Classification System)	0.075 to 4.75

2.1.1 Natural Sand

Natural sand generally contains particles formed from quartz and feldspar. Grains formed from other minerals such as calcite, mica and fragments of limestone, slate and basalt can also be found (Das, 2008). Feldspars formulate around 60% of the earth's crust and are the popular components in crystalline rocks (Kyonka & Cook, 1954). Feldspars are commonly white or light coloured (Shakkour, Rabb, & Sadeq, 2015). Sand containing a high amount of quartz is referred to as silica sand. Quartz can be seen as natural silica. It is mainly clear, but can be white in colour or could be bright coloured because of some mineral contents (Barrett & Beskeen, 1986).

The most common way of grain sorting in sand is when water carries grains. The water dumps the heavier, larger particles at the bottom first followed the lighter, smaller particles on top. Well-sorted sand contains particles within one or two size level (Barrett & Beskeen, 1986).

Sand particles originally come from rocks, created by erosion action. After getting broken off from its source, the resulting particles are then transported by water, ice or wind to lakes, rivers, sea or sand dunes. The sand particles are further reworked after deposition, by infiltration and movement of surface water and other factors such as leaching/disintegration, consolidation, cementation, and weathering. These factors also affect the mineral composition of sand which could vary according to different locations. Further transportation of particles will help determine the shape, size and mineral composition (Pinard et al., 2013). This process is illustrated in Figures 2.1 and 2.2.

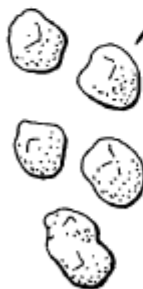
PATH OF A SAND GRAIN

Minerals such as quartz, mica, feldspar bound up as part of a rock.



Rock is broken down and sharp-edged fragments drop off. These are **ANGULAR** fragments.

Fragments strike each other as water or wind, ice or gravity move them downhill. Most sharp edges are worn away. These are **SUBANGULAR** fragments.



Running water or winds continue to batter the rock particles. Most sharp edges are smoothed down. The particles are **SUB-ROUNDED**.

When all the edges are worn away and the surface is very smooth the grains become **ROUNDED**.



Figure 2.1: Stages of sand particle formation (Barrett & Beskeen, 1986)

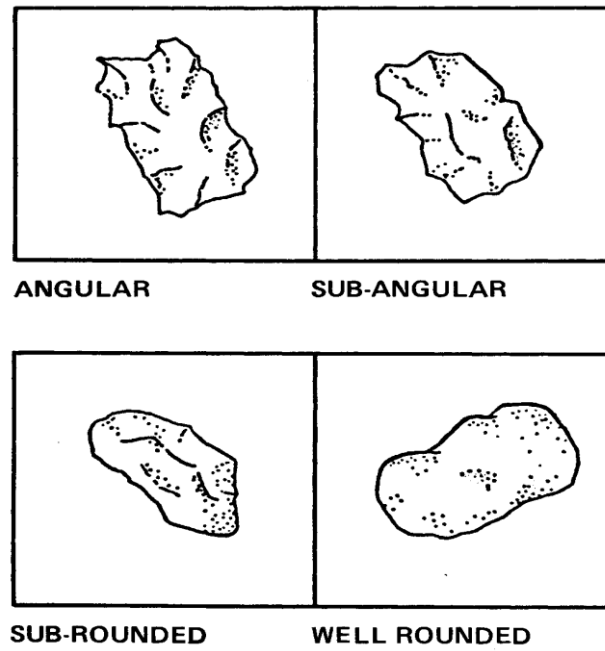


Figure 2.2: Shapes of sand particles (Barrett & Beskeen, 1986)

Sands and sandstones can be used for aggregate in concrete, sand fills, building stone, moulding in foundries, glass sand, abrasive, sand filters and metal (Heinrich, 2001).

2.1.2. Sandstone

Sandstone is a term referred to sand that has been lithified over time into a rock mass. It is used only in the case of siliciclastic rocks (i.e. they contain sands that are made from silica and quartz) and not for carbonate rocks (rocks that original from fossil). Sandstones are formed when sand grains get compressed over time until the become a rock, which can contain cementing substances that are deposited after seeping water dries out. Sandstones can be carved into blocks that can be used in construction as seen in Figure 2.3 (Southard, 2007).



Figure 2.3: Blocks of carved sandstone at Serhatköy, North Cyprus

2.1.3. Crushed Sand

Crushed sand can be found abundantly in limestone quarries and utilising it could decrease cost of concrete while helping with disposal cost and environmental pollution (Menadi et al., 2009). There has been a shift towards crushed sand due to increased construction activities because of global economic development (Kim et al., 1997). Crushed sand of particles below 5mm forms as a by-product during the crushing of coarse aggregate needed for transportation infrastructure. It is different from natural sand in grain distribution, shape, surface texture and fine contents (Zoubir et al., 2014). These properties have shown in researches that crushed sand can be used in concrete without showing any change in its characteristics. Even limestone fine content of up to 15% does not affect the strength of concrete (Menadi et al., 2009). However, Celik and Marar (1996) discovered that the higher fine content decreased the slump, air content and permeability of the concrete. Crushed sand however, needs more mixing water than normal silica sand in order to reach a certain fresh behaviour (Zoubir et al., 2014). There is also no difference in concrete behaviour with relation to temperature

when crushed sand is used (Choi & Choi, 2013). Crushed sand with higher fine content increase the modulus of elasticity of concrete, making it more elastic (Carlos et al, 2010).

2.2 Shear Strength

The shear strength of soil is considered very significant for the design and analysis of geotechnical structures. Laboratory or field tests can be conducted to obtain results for the Mohr–Coulomb parameters for shear strength analysis of soil (Zhou et al., 2016).

Shear strength of soil can be defined as “the internal resistance per unit area that the soil can pose along a plane within it before yielding”. The usual shear strength parameters include internal friction and cohesion. The internal angle of friction, ϕ , is brought about by the interlocking of the soil particles (Adunoye, 2014). Cohesion, c , is defined as the value of shear strength at zero normal stress along the failure. It can be seen as the resistance caused by the forces that grip together the soil particles into a solid mass (Alias et al., 2014) However, for dry sands, we should note that $\sigma = \sigma'$ and $c' = 0$ (Adunoye, 2014). However, unsaturated sand can show some cohesion even though the effective cohesion is still zero (Farouk et al., 2004). Soil physics defines cohesion to be the force of cohesion that is present between particles. As for soil mechanics, cohesion is the value of shear strength when compressive stresses are at zero (Adunoye, 2014).

Mohr came up with a concept for rupture in components material in the year 1900. In his theory, he stated that important combination of shear and normal stresses causes failure across a plane in a given material. This combination can be given as the function in equation 1.

$$\tau=f(\sigma) \tag{1}$$

where,

τ = the shear stress at failure and

σ = the normal stress on the failure plane.

Earlier in 1776, Coulomb stated the function $f(\sigma)$ as equation 2 below.

$$\tau=c+\sigma \tan\phi \tag{2}$$

where,

c = the cohesion is the intercept on the shear stress axis

σ = the normal stress on the failure plane.

ϕ = the friction angle or angle of shearing resistance indicates the slope of the line.

Dafalla (2013) stated that Direct Shear Test (DST) can be applied on clay-sand soil liner materials as long as the material is not placed within CL groups according to ASTM D 2487 or BS 5930. British standards consider a soil clay when the clayey material is 35% or more. The ASTM however, consider a soil sample as clay when 50% passing the no. 200 sieve is clay. The DST is more suitable for granular soil materials. The DST apparatus is illustrated in Figure 2.4.

Fu et al. (2015) stated that all parameters of Mohr-Coulomb theory (internal friction angle and cohesion parameters) can be evaluated from DST or Triaxial Compression Test. They also back the point that DST is more convenient for its convenience, simplicity and shorter

duration. The apparatus for DST is easy to operate and it gives data output that can be easily processed to calculate shear strength parameters (Alias et al., 2014).

It has been extensively stated that several factors affect the shear strength of soil. These include, the kind of soil, grain composition, rock origin of soil particles, compactness, environmental conditions (such as variation in water content, stress state, disturbance and seepage), test method and particle shape (Fu et al, 2015). Dafalla (2013) also pointed out in his experiment the drop in shear strength resulting from increasing the moisture content under the different normal stress values.

The size of particles present in the soil sample causes differences in strength behaviour. Increasing the particle size to not more than 10mm causes a decrease in friction angle; however, particles with maximum 75mm of grain size show higher friction angle than particles with maximum 10mm grain size by up to 3 degrees (Alias et al., 2014). Fu et al, (2015) stated that Coarse-grained soil is well known for its excellent resistance against shear and has been widely used in geotechnical engineering projects such as foundations, earth-filled dams, embankments, and breakwaters.

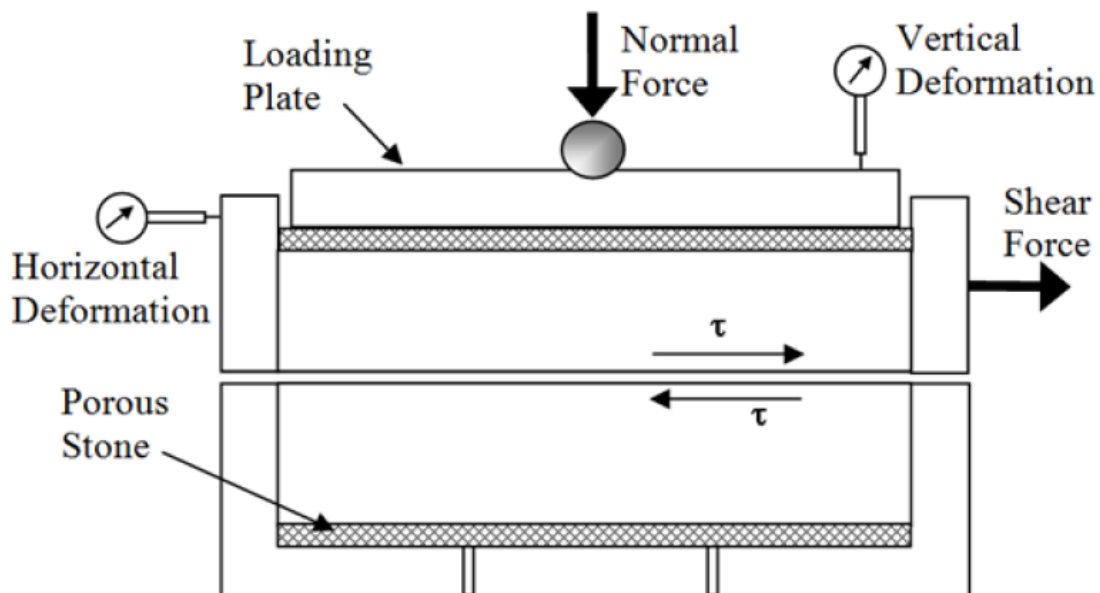


Figure 2.4: Diagram of direct shear test arrangement (Das and Sobhan, 2012)

However, the direct shear test has its own limitations. The programmed horizontal failure plane employed by the apparatus may not essentially be the weakest plane of the sample. Secondly, the stress is higher towards the edges of the shear surface than at the middle, which implies uneven spreading of the stress (Das, 2008).

2.2.1 Mohr's Circle

The Mohr-Coulomb failure envelope is generated by placing a straight line fitting the points showing the results from the experiment (illustrated in Figure 2.5). The angle of the line represents the peak angle of friction of the tested soil. The line is plotted on the graph of shear stress versus normal stress (Das, 2008). Examples of friction angles are given in Table 2.2.

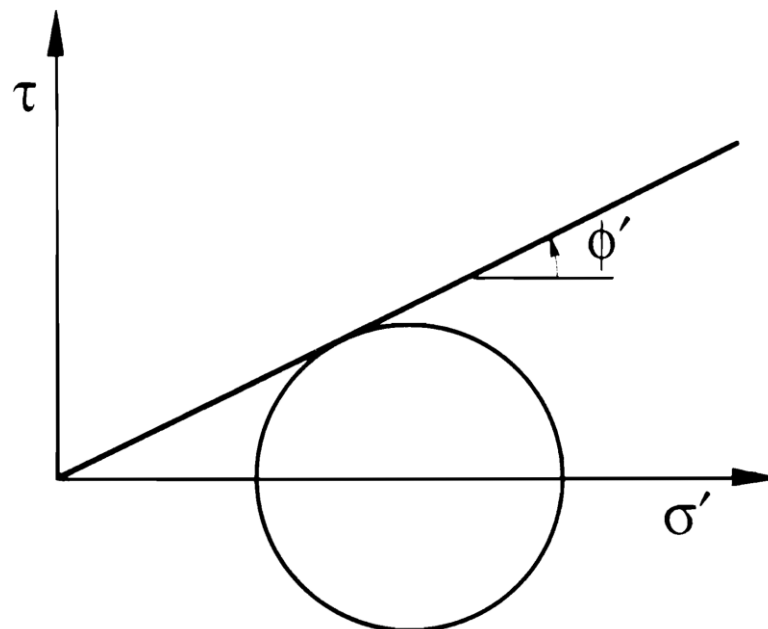


Figure 2.5: The Mohr-Coulomb failure criterion (Houlsby, 1991)

The common pattern of shear stress against horizontal displacement plot indicates the same bilinear profile over different normal stresses. The shear moduli at initial stage, before the critical shear, and beyond the critical shear value can all be computed (Dafalla, 2013).

Table 2.2: Common values of friction angle of silts and sands (Terzaghi and Peck, 1967)

Material	Friction Angle (degrees)
Sand, Uniform, round grains	27-34
Sand, well graded, angular	33-45
Sandy gravels	35-50
Silty sand	27-34
Inorganic	27-35

2.2.2 Normal and Shear Stresses

The normal force (applied in equation 3) used in DST can be obtained from the mass applied during the test. Shear stress is evaluated using equation 4.

$$\sigma = \text{Normal Stress} = \frac{\text{Normal force}}{\text{Cross-sectional area of the specimen}} \quad (3)$$

The Shear stress can be evaluated using

$$\tau = \frac{\text{Resisting shear force}}{\text{Cross-sectional area of the specimen}} \quad (4)$$

Regarding the DST however, the gap between shear box halves and specimen size, which can be summarized as the scale effect, may be two important factors affecting shear strength of a specific coarse-grained soil sample. The scale dependence of the internal friction angle of cohesion-less soil sample, observing that the larger the direct shear box, the smaller the

internal friction angle. Results showed that the gap effect under a large normal stress is stronger than that under the small one (Fu et al, 2015).

Dafalla (2013) pointed out that shear stress against horizontal displacement plot demonstrates a general bilinear plot for normal stress values all inside the elastic zone. Plastic softening is noticed close to the value of critical shear, and the shear stress versus horizontal displacement gradient flattens and signifies a fall in the shear stress across a wide horizontal displacement in comparison to the elastic zone.

2.2.3 Dilation

Dilation means change in the volume of granular samples caused by shearing. It was defined and detected by Reynolds in 1885. Initial researches focused on strain-stress curves gotten from simple shear tests. The curves also show the value of angle of friction that relates to residual stress after failure and maximum shear stress. It is commonly known in soil mechanics that angle of friction is the total of the angle of dilation with angle of friction at constant volume. The occurrence of dilation is linked with the “dissipation of work in frictional soil” (Sawicki, 2014).

We can measure vertical and horizontal displacements of soil during shear to note the dilation in the soil, i.e. increase in volume as demonstrated in Figure 2.6. A very important factor affecting dilation is the density of the soil, with denser soil sample showing more dilation (Houlsby, 1991)

Simoni and Houlsby (2006) stated the introducing gravel particles to the sample, even as low as lower than 10% volume, produced a rise in peak angle of friction caused by increased dilation.

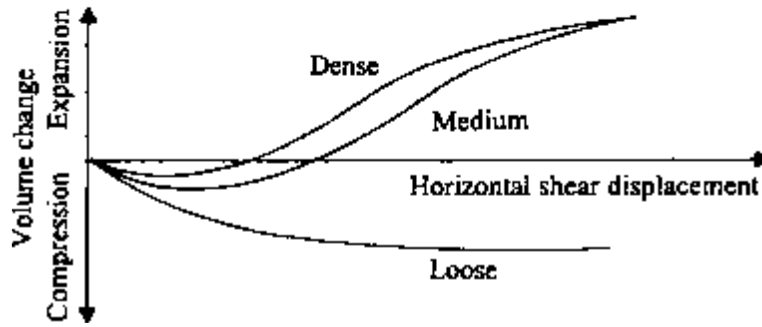


Figure 2.6: The of graph soil displacement during shearing (Das, 2008)

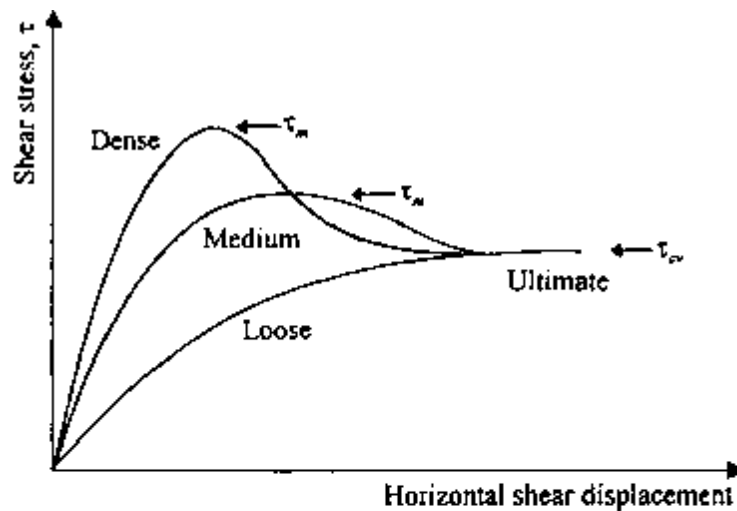


Figure 2.7: Direct shear test results in loose, medium, and dense sands (Das, 2008)

1. Regarding dense and medium sands, the shear stress rises in conjunction with shear displacement to reach peak value before coming down to a steady value at high displacements. This is referred to as the ultimate shear stress.
2. While in loose sands, we find that shear stress rises as shear displacement rises to a peak level and keeps constant.
3. Volume of dense and medium sands initially decreases before increasing in tandem with shear displacement. However, the volume remains the same at higher shear displacement values.

4. Volume of loose sands slowly decreases to a certain level and then stays constant therefrom (Das, 2008).

The different patterns of the horizontal displacement vs shear stress curves for the above listed states of sand density can be seen in Figure 2.7 (Das, 2008)

2.3 Suction in Unsaturated Soil

In the late 1800s, agronomists and soil physicists initiated basic research associated with the importance of pore fluid found in soils which was later utilised in engineering. The work done by Cronney et al. in England between 1948 and 1950 was probably the premier research to acknowledge the importance of suction in civil engineering. They used terminology adopted from soil science and noted the change in soil behaviour caused by change in soil moisture. Later researchers managed to integrate soil suction into an equation of effective stress that demonstrated changes in shear strength and volume of soil (Krahn & Fredlund, 1972).

The simultaneous improvements in theoretical and experimental analyses have led to increased research in unsaturated soil mechanics in recent decades. It should probably be noted that geotechnical engineers started their researches in unsaturated soil with important contributions from experts in Soil Science, with focus on water transfer and water retention. During that period, geotechnical engineers began investigation into water retention characteristics of soil and early researches were conducted in 1961 (Delage, 2008).

International Society of Soil Science quoted definitions of suction adopted by the Soil Mechanics Symposium Panel (Moisture Equilibria and Moisture Changes in Soils). They defined Total Suction to be the sum of matric suction and Osmotic suction. It may also be calculated by the measurement of the vapour pressure with soil water (Krahn & Fredlund, 1972).

Matric Suction may be defined as the negative pressure in relation to gas pressure acting externally on the soil sample, which must be exerted on a solution that has similar components as the soil water so as to reach a state of equilibrium, via a porous wall, with the soil water (Çokça & Tilgen, 2010). In general, matric suction is linked with the capillary rise caused by surface tension of water (Elgab, 2013).

The presence of dissolved salt causes reduction in relative humidity; this is referred to as Osmotic Suction. Osmotic Suction is also defined as the negative pressure that is exerted on a pool of water so as to reach equilibrium, via a semipermeable membrane, with a pool of solution that has similar components with the soil water (Çokça & Tilgen, 2010).

Total Suction is defined as the negative pressure in respect to gas pressure acting externally on the soil water, which must be exerted on a pool of pore water so as to reach equilibrium with the soil water via a semipermeable membrane. It is the sum of matric (soil water) suction and osmotic suction (Krahn & Fredlund, 1972).

Wetting suction process absorbs lower water content than drying process due to a phenomenon referred to as 'ink-bottle effect' (See Figure 2.12). Uneven distribution of pore size has geometrical effects that cause creation of air bubbles in dead-end during wetting, hence the difference between wetting and drying processes (Song, 2014).

2.3.1 Suction Measurement Methods

There are two classifications of suction measurement; direct or indirect. The direct measurement techniques aim at observing pore-water pressure, while indirect techniques aim at measuring other soil properties related to suction using a determined value of suction. Such values include water content, relative humidity and resistivity (Elgab, 2013).

Tube Suction Test

It is used to measure the moisture absorption of granular materials. This apparatus was developed by the Finnish National Road Administration in 1994. The usual setup used for this method calculates moisture susceptibility of soil samples by means of dielectric values measured using electric probes (see Figure 2.8) or a percometer. Higher dielectric values are connected with matric suction, and indicate higher moisture susceptibility and moisture content (Kassem et al. 2009). It is based on the capillary rise concept (Figure 2.9) initially suggested by Lambe (1982). The TST also owes its concept to infiltration where a tensiometer-transducer can be employed to compute the pore-water pressure of the soil sample present in the tube. A ceramic cup can also be used to measure pore-air pressure through holes in the tube (Yang et al., 2004).



Figure 2.8: TST Setup with electric probes (Monash University, 2017)

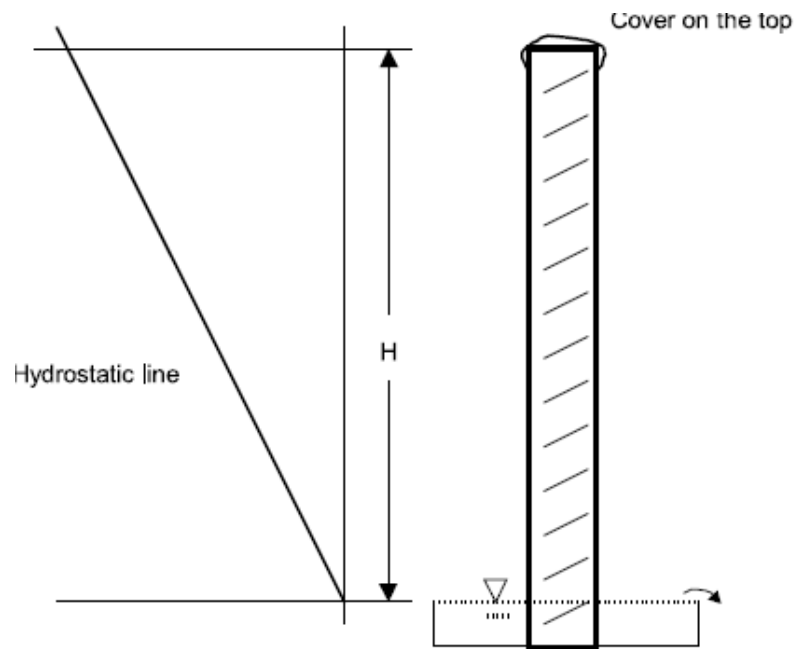


Figure 2.9: Diagram illustrating capillary rise (Yang et al, 2004)

Tensiometers and High Suction Tensiometers Tests

The tensiometer is governed by a basic principle that once the tensiometer and the soil reach pressure equilibrium, the tension on the water present in the tensiometer will be equal to the negative soil pore-water pressure. This technique is, however, limited to about 100 kPa because of cavitation issues (Lourenço et al., 2006). Osmotic suction cannot be measured due to the absence of semi-permeable membrane used for soluble salt (Pan et al., 2010)

A tube filled with deaired water is fitted with a small ceramic cup and attached to a pressure sensor. Filling the ceramic cup with water and applying vacuum to it makes it saturated. Reduce water pressure present in the sensor by leaving the ceramic tip to dry. Tensiometer measurement range cannot be raised by the introduction of ceramic cup of higher air entry because of the problem of cavitation (Pan et al, 2010).

Improvements have been made to create High Capacity Tensiometer (HCT) that can now measure matric suction up to 1500 kPa (Lourenço et al., 2006). However, there are limitations that could result from the air in the sensor causing a low or negative value of the pore water pressure (Toker, 2002).

Thermal conductivity sensors test

Thermal conductivity sensor (TCS) was introduced by Shaw & Baver (1939) as an equipment for matric suction measurement (Fredlund & Wong, 1989). It uses a ceramic porous block as a means to measure matric suction. The main idea behind the test is if there is difference in matric suction between the porous block and the soil, water transfer will occur until suction reaches equilibrium. The thermal conductivity of the fluid and the solid present in the voids within the porous block constitute the thermal conductivity of the block (Marjerison et al., 2001). The thermal conductivity of the block goes up as the moisture content in the block goes up. The moisture content can be measured by recording the temperature rise of the porous block during heating, which is done using a heater implanted in the middle of the block. The moisture content and the temperature rise can be used as means of measuring matric suction in the soil. TCS can be used both in the laboratory as well as on the field (Nichol et al., 2003).

TCS can give reliable measurements of a wide range of soil suction which are not affected by the presence of salt in the soil (Lee & Fredlund, 1984). The device can also be connected to a remote monitor and data acquisition system. However, the TCS is susceptible to durability issues from the ceramic tip and low stability of electronic signals. It also shows sensitivity to the porous block from one device to another, begging for different calibration curve for each thermal conductivity sensor (Pan et al., 2010).

Electrical conductivity sensors test

The electrical conductivity sensor has a porous block with two concentric electrodes implanted in the block. The electrical resistance of the block decreases as its moisture content increases. The matric suction of the block is connected to its electrical resistance. The number of electrical conductivity readings obtained in the field can be limited because they are obtained manually (Skinner et al., 1997). Gypsum is the most suitable material used as porous block because it saturates the quickest, although it can damage the electrical conductivity sensors because the gypsum will ultimately dissolve into the soil. The electrical conductivity sensor takes a long time to reach equilibrium when there is fast change in moisture content. The matric suction equilibration time ranges from 6 hours for 50 kPa matric suction to 50 hours in the case of 1500 kPa of matric suction (Pan et al, 2010). However, the sensors become less sensitive at suction levels beyond 300 kPa. Moreover, salt content of the soil could affect the sensitivity of the electrical conductivity sensors which may not necessarily indicate the moisture content of the porous block (Skinner et al., 1997).

Null-type Axis-translation technique

Null-type axis-translation apparatus is used for measuring matric suction of unsaturated soil based on the axis-translation technique. The axis-translation technique was primarily invented to surpass the issue of cavitation at low water pressures. A porous material is normally employed as a means to attain axis-translation by sorting out water and air phases in the soil. The porous material commonly used is ceramic disk. Since the ceramic disk is saturated, it only allows water passage and not free air when suction is being applied (Kurucuk et al., 2012).

The value of air-entry in the ceramic disk limits the matric suction readings when this technique is used. This technique gets its name because the pressure in the water compartment is always kept at zero. Pore-water pressure will increase whenever there is an increase in applied air pressure, provided the mass of water remains constant. This means

the matric suction remains the same irrespective of pore-air and pore-water pressures translations (Elgabu, 2013).

Time domain reflectometry technique

Time domain reflectometry (TDR) is a technique initially introduced by Topp et al., (1980) as a method for evaluating volumetric water content in soils. The dielectric constant in the soil which is linked to volumetric water content is evaluated using TDR (see Figure 2.10) (Yu & Drnevich, 2004). TDR measures matric suction and not total suction because it measures capillary rise resulting from bulk pore-water present in soil pores. Soil-water characteristic curve is needed to correlate the matric suction to the obtained water content. This technique is suitable for providing reliable values of volumetric water content within a short period of time. However, it may demand very complex electronic setup (Benson & Bosscher, 1999).

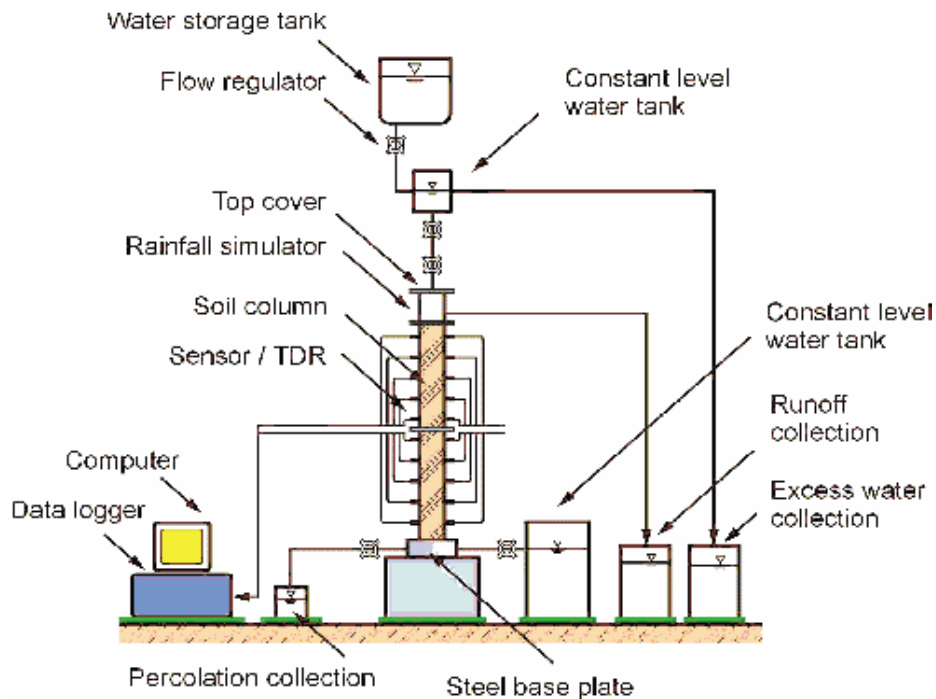


Figure 2.10: A full setup of a TDR test (Yang et al, 2004)

Filter paper method

This cheap, easy and accurate method can be used to measure both total and matric suctions (Leong et al., 2003). The idea is for the filter paper to reach equilibrium with the soil by means of liquid or vapour fluid flow, which would also mean a constant suction value of the filter paper (Bulut et al., 2001). The method's principle relies on relating suction with the water soaked up by the filter paper using calibration curves (Al-Khafaf & Hanks, 1974). Total suction can be determined since the moisture movement occurs through vapour movement when filter paper and soil specimen are detached from each other. Matric suction is determined when there is direct contact between the filter paper and soil specimen, where the moisture movement is by means of liquid flow. Osmotic suction can be determined with the non-contact technique as illustrated in Figure 2.11 (Elgabru, 2013).

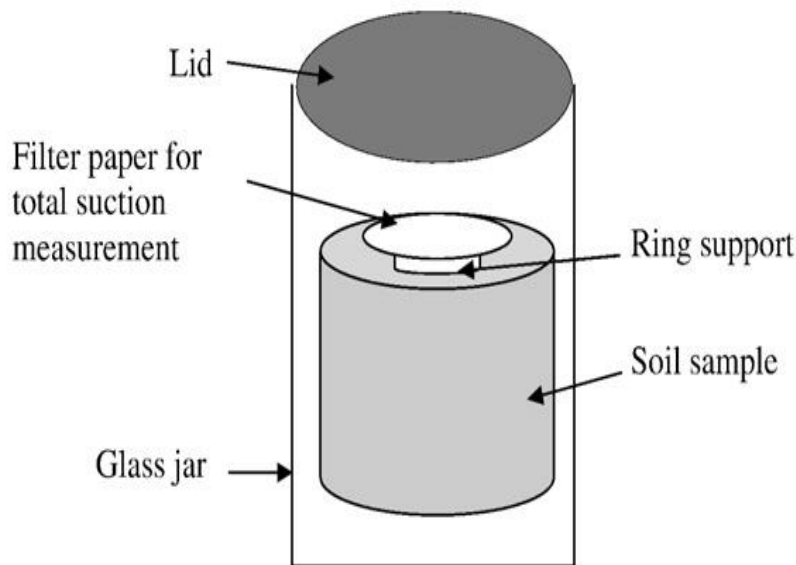


Figure 2.11: A diagram of non-contact filter paper technique (Çokça & Tilgen, 2010)

The resultant suction value is determined from the calibration curve of water content against suction, meaning that the filter paper method is classed as an indirect method for determining soil suction. The ASTM D 5298-92 (Standard test method for measurement of soil potential (suction) using filter paper in soil suction measurements) provides the calibration curves for various filter papers (Çokça & Tilgen, 2010).

Psychrometer test

The Thermocouple psychrometer and the thermistor or transistor psychrometer are the most common types of psychrometer. The thermocouple psychrometer was presented by Spanner (1951). It is based on Peltier and Seebeck effects. The Peltier effect happens when temperature decreases as a result of electrical current moving through a junction of two separate metal wires, which is a result of relative humidity of the environment where measurement is ran. The thermistor or transistor psychrometer was invented by Richards (1965), and it is made up of an insulated container that has the psychrometer probes and a data logger meant for computing output. The transistor psychrometer uses an electronic wet and dry bulb thermometer. The total suction is taken as the voltage output from the wet and dry transistors. The total suction value ranges from 100 to 10,000 kPa (Tang et al., 2002).

The transistor psychrometer has replaced the thermocouple psychrometer in most laboratory because it has been improved with micro-chip technology (Woodburn et al., 1993). However, the accuracy of the transistor psychrometer at high suction values is affected by changes in electromotive force (Ridley & Wray, 1996). Also, the psychrometer may become insensitive because of temperature change. There may also be deterioration caused by corrosion (Zerhouni, 1995).

Chilled-mirror hygrometer test

The theory behind the chilled-mirror hygrometer device is in accordance with Kelvin's equation, established on the relationship between temperature, relative humidity and total suction (Agus & Schanz, 2005). The chilled-mirror hygrometer measures total suction according to the equilibrium of the liquid form of water in the soil specimen with the vapour form in the air void on top of the soil sample. It is quick and simple to measure suction using the chilled-mirror hygrometer (Pan et al., 2010)

Relative humidity probe test

Temperature and relative humidity of vapour present in soil sample can be used to calculate total suction through the use of Kelvin's law (Fredlund & Rahardjo, 1993). Polymer capacitance sensor has been introduced as a means to measure the relative humidity in soil samples. This sensor has a thermoset polymer film that separates two electrodes. The thermoset film releases water or absorbs it according to the relative humidity value being recorded. Polymer capacitance technology provides a quick and reliable way of measuring relative humidity with low hysteresis and low response to temperature change during measurement (Benson & Bosscher, 1999; Wiederhold, 1997).

Table 2.3: The summary of different methods and techniques for measuring suction

Method	Suction Component	Range (kPa)	Duration	Remarks
Tensiometers	Matric	0-90	Minutes	Direct. Daily attention must be paid to prevent cavitation
High suction Tensiometers	Matric	0-1500	Minutes	Direct. Cavitation may occur at high suction by air diffusion through ceramic cup
Tube suction	Matric	0-100	5-7 days	Indirect. Different sizes of tube affect duration.
Thermal conductivity sensors	Matric	10-1500	Few hours- few days	Indirect Sensitive to temperature
Electrical conductivity sensors	Matric	10-1500	Few hours- few days	Indirect. Sensitive to temperature and salinity of soil water
Null-type axis-translation	Matric	0-1500	1-16 hours	Direct. Ceramic disk air-entry value is limited
Time domain reflectometry	Matric	0-500	Instant	Indirect. Requires expensive equipment
Filter Paper	Matric	0-1000	2-5 days	Indirect. Depends on equilibrium time and calibration curve, cheaper
	Total	Above 1000	3-14 days	
Psychrometers	Total	100-10000	5-10 hours	Indirect. Sensitive to temperature
Chilled-mirror Hygrometer	Total	100-300000	3-20 minutes	Indirect. Inaccuracies at lower suction values
Relative Humidity probes	Total	Above 1000	Few minutes- hours	Indirect. Sensitive to temperature, difference in accuracy due manufacturer

2.4 Soil-Water Characteristics Curve (SWCC)

Soil physicists have essentially used the SWCC in agriculture to obtain the water storage properties of soils close to the ground water, while engineers have used it in soil mechanics to estimate the characteristics of unsaturated soil to further solve the numerical modelling problems encountered in geotechnical engineering. However, both parties have mainly treated the SWCC as a mere relationship between water content and soil suction. They've both also considered disturbance of the soil sample as unimportant, allowing for reshaping and remoulding of samples in laboratory tests (Fredlund & Houston, 2013). A Soil-Water Characteristics Curve (SWCC) can be defined as the variations in the degree of saturation or water content in relation to suction (See Figure. 2.12) (Vanapalli et al., 1996).

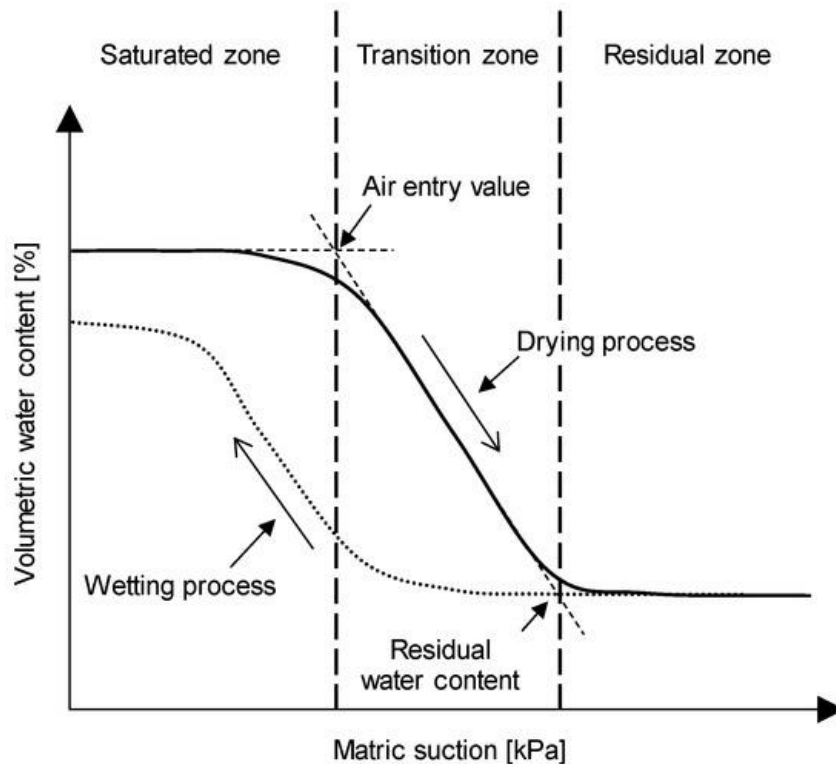


Figure 2.12: An example of SWCC (Hong et al. , 2016)

There has been increased interest in the available measurement procedures for finding the correlation between the suction and water content from researchers in the field of geotechnical engineering. Experts in geotechnical engineering have different application of

the SWCC from experts of agriculture. This is because geotechnical engineers have interest in soil swelling in relation to suction, caused by loading and wetting. Their primary use of the SWCC has been to evaluate properties of unsaturated soil against suction, including shear strength and permeability (Fredlund & Houston, 2013). SWCC has also been related with soil properties such as grain size, soil microstructure, density, plasticity, water content, degree of saturation and dry unit weight (Delage, 2008)

In their research, Fredlund and Houston (2013), discovered that interpretation of information obtained from SWCC can be affected by changes in volume of soil sample as increase in suction occurs. They conducted their test on samples of Oil Sand Tailings and Regina Clay.

Delage (2008) pointed out that SWCC (or WRC- Water Retention Curve) can also be correlated with shear strength due to the fact that SWCC provides information on the inter-particle contact and stresses at different suctions. This is suitable for sandy soil where we can observe contact between soil particles.

Fredlund and Xing (1994) fit Model

The Fredlund and Xing (1994) SWCC modelling equation is used to estimate the SWCC of any soil samples having separate void ratios. It should be considered that these samples may have similar residual suction and water content, while the air entry value differs linearly. The Fredlund and Xing (1994) model (represented by equation 5) uses different soil parameters to successfully model the SWCC of a soil (Gao & Sun, 2017).

$$\theta = \left(1 - \frac{\ln\left(1 + \frac{\psi}{\psi_r}\right)}{\ln\left(1 + \frac{10000000}{\psi_r}\right)} \right) \left(\frac{\theta_s}{\left(\ln\left(e + \left(\frac{\psi}{a}\right)^n\right)\right)^m} \right) \quad (5)$$

Where:

- θ = volumetric water content at specific suction
- θ_s = saturated volumetric water content.
- Ψ = highest soil suction
- Ψ_r = soil suction matching with the residual water content
- α, n, m = fitting parameters
- e = Euler's number

Van Genuchten (1980) fit Model

In 1964, Brooks and Corey came up with mathematical function that can be used to explain moisture release gradient. The function was further improved as a model by scientists such as Campbell (1974), Gregson et al. (1987) and Williams et al. (1992). These scientists further introduced soil characteristics parameters such as saturated water content at zero matric suction, as well as a and b parameters (Meissner, 2004). In 1980, van Genuchten suggested a model and introduced parameters such as n (seen in equation 6) (Sheng et al., 2008).

$$\theta = \theta_r + \frac{\theta_s - \theta_r}{[1 + (\alpha\psi)^n]^m} \quad (6)$$

Where:

- θ = water content of soil
- θ_r and θ_s = water content of soil at dried and saturated conditions respectively
- ψ = highest value of pressure head of soil water
- α, n and m = parameters determined by fitting the equation to experimental data and assuming $m = 1 - 1/n$

The values of α , n and m can be obtained using software programs such as SoilVision or RETC (Ghanbarian-Alavijeh et al., 2010).

Van Genuchten (1980) equation has been found out to be applicable for most soil textures. It is paramount to find out the difference between the estimated values and the measured values from the experiment. This could be done by the use of R^2 (determination coefficient) (Yang & You, 2013). This coefficient can be calculate using equation 7 below.

$$R^2 = 1 - \frac{\sum_{i=1}^N (M_i - P_i)^2}{\sum_{i=1}^N (M_i - \bar{M})^2} \quad (7)$$

Where:

P_i and M_i = estimated and measured values of the i -th measured data respectively

\bar{M} = mean of the measured values.

Air Entry Value and Residual Water Content

Air entry value is the value of matric suction which should be exceeded before air moves back into the soil pores (Aldaood et al., 2014). This is the pressure head at which water starts to be displaced by air in a porous medium. On the opposite side, the water entry value is the lowest pressure head at which water can seep into the soil. This means that the water entry is involved in infiltration while air entry is involved in drainage (Konyai et al., 2009).

The residual water content corresponds with the residual zone, which is the point at which the soil begins to desaturate. The matric suction at this point can also be noted (Zhai et al., 2017).

CHAPTER 3

METHODOLOGY

3.1 Samples

The natural sand was retrieved from Gaziveren (GAZ). It is a natural sea sand deposited from weathered materials from Trodos Mountains. It is grey brown in colour and contains pieces of coral and marine debris as seen in Figures 3.1 and 3.2. It is classified as SP (Poorly graded with little fines) under the USCS classification.



Figure 3.1: A sample of GAZ used in the laboratory



Figure 3.2: Huge deposit of GAZ sand

Gürdal (GÜR) and the Roadworks Department Quarry (RDQ) samples were crushed sands that were initially just by-products of coarse aggregates crushing (refer to Figures 3.3 A & B). They are crushed from dolomitic limestone (see Figures 3.4 A & B) containing trace of magnesium and have the same grey colour as the parent rock. GÜR is classified as SW-SM (Well graded silty sand), while RDQ was SP-SM (Poorly graded silty sand).



Figure 3.3: Sample of GÜR (a) and RDQ (b) used in the laboratory



(a)

(b)

Figure 3.4: The parent rock and crushed sand deposit for RDQ (a) and GÜR (b)

Serhatköy (SER) sample was crushed yellow sandstone produced as a product of sandstone mining (Figure 3.5). The sample can be seen as a cross between crushed and natural sand seeing as sandstone itself is formed from natural sand (Figure 3.6). SER is Poorly graded silty sand (SP-SM).



Figure 3.5: A sample of SER used in the laboratory



Figure 3.6: Yellow sand deposit from sandstone mine (SER)

Basic properties of the soil samples were examined, including grain-size distribution, specific gravity, and minimum and maximum densities and void ratios. All these tests were performed under respective ASTM guidelines. Samples were oven dried and cleaned to prepare for the laboratory tests. The Gaziveren sample contained pieces of dead coral that had to be sieved out.

The sieve analysis was conducted on the four samples according to ASTM D422 to find out the gravel, sand and fine contents. The sieve analysis results were then used to classify the soil sample under Unified Soil Classification System (USCS). According to ASTM D422, particles retained in the #4 (4.75mm) sieve are classified as Gravel particles, while particles retained in the #200 (0.075mm) are classified as Sand particles. Particles that pass through the #200 sieve are classified as Silt/Clay. The full set of sieves used can be seen in Table 3.1.

Table 3.1: Sieve number and sizes used in the sieve analysis of the soil samples

Sieve Number	Diameter (mm)
#4	4.75
#8	2.36
#10	2.00
#20	0.85
#30	0.60
#40	0.43
#50	0.30
#100	0.15
#200	0.075
Pan	-

Tests for specific gravity were conducted according to ASTM D854. The samples were oven dried before use in this test. The setup for specific gravity test can be seen in Figure 3.7



Figure 3.7: The setup for specific gravity test in the laboratory

The relative density was conducted according to ASTM D4253-16 using a metal mould of 11.5cm depth and a diameter of 10.2cm. the mould weighed 4072g. The mould can be seen set up on the agitating table in Figure 3.8.



Figure 3.8: Shaking table used for relative density test

Atterberg limits tests were hindered due to lack of cohesion from the sand samples. Some samples may contain fine contents of up to 11% (like GÜR), but the fine particles do not show any clayey properties. SER however showed plasticity and was tested successfully for Atterberg limits test.

3.2 Tube Suction Test (TST)

To conduct the wetting experiment, the tube loaded with soil sample is placed in water kept at a level below the bottom extraction hole. The soil was loaded into the tube up to maximum density which was achieved by agitating the tube and use of a tamping rod. The maximum density was found using the relative density test. The drying procedure is done by supplying water at the top of the soil sample flowing downwards. The water supply is stopped when the soil becomes saturated and that is when the drying begins. We can know that the soil is saturated when there is water dripping from the bottom. The total soaking time for the drying suction was 7 days while the wetting suction also took 7 days. The sample was retrieved from the tube through the holes at different heights of suction. The setup used in this research can measure matric suction of up to 100 kPa.

The tube was 8.2cm in diameter and with a total height of 110cm. there are sample retrieval holes 10cm apart from the bottom to a height of 100cm on the tube. The holes were covered with tape to prevent sample loss as seen in Figure 3.9. A porous stone was placed at the bottom of the tube to facilitate water transfer. Filter paper was placed at the bottom before the sand was loaded to prevent sample loss. The tubes were elevated above the bucket floor by means of blocks 5cm high.



Figure 3.9: The soil tube place in a bucket of water after loading samples. Retrieval holes have been covered with tapes to prevent sample loss

3.3 Direct Shear Test (DST)

Direct Shear Test: It was conducted using the Direct Shear Apparatus (Figure 3.10) available in the laboratory in accordance with the ASTM D 3080-03 standard procedure. The sand

specimens were tested at maximum density. The samples were sheared in their highest density (from the relative density test) state under normal stress values of 27.8 kPa, 55.6 kPa and 83.3 kPa. The normal stress is derived from the normal weight applied on the lever arm hanger. This normal force is divided by the area of the of the shear box to give the normal stress (see equation 3). The normal force applied is 100N, 200N and 300N respectively. The test was conducted on the sands at three different moisture contents. The shearing was done under drained conditions with the use of a porous stone. The apparatus has a square shear box with dimension $6 \times 6 \times 1$ cm. The rate of shearing for all samples was 0.1mm/min. The results and graphs from the test were plotted automatically by the device and retrieved using a computer software.



Figure 3.10: DST setup used in the laboratory

SWCC was drawn using suction calculated from the suction formula and also using the SoilVison computer Program, which helps in fitting the prediction models of Fredlund and Xing (1994) and van Genuchten (1980).

CHAPTER 4

RESULTS AND DISCUSSIONS

4.1 Samples

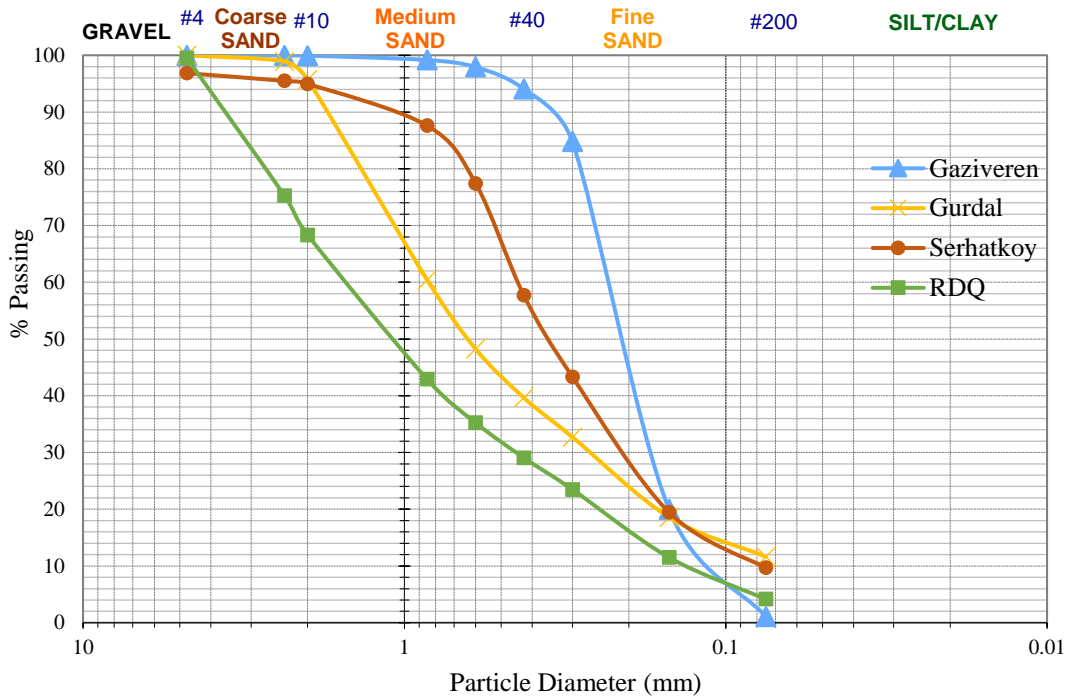


Figure 4.1: Particle size distribution curve of the four samples

The Gaziveren sample falls under the SP (Poorly graded with little fines) classification. That is because it contains 0% gravel, 98.83% sand and 1.17% fines.

The Gürdal sand was classified as SW-SM (Well graded silty sand). Serhatköy SP-SM (Poorly graded silty sand). There were no gravel particles present while it contained 88.85% sand and a fines content of 11.15%.

The Serhatköy sample is classified as SP-SM (Poorly graded silty sand). It contains 3.160% gravel, 87.55% sand while having 9.29% fine content.

According to the USCS classification, the RDQ sand was classified as SW (Well Graded with little fine). It contained 0.51% gravel, 95.3% sand and 4.19% fine particles.

Table 4.1: Physical properties of soil samples

Sample	ASTM STANDARDS	GAZ	GÜR	SER	RDQ
Specific Gravity	ASTM D854	2.70	2.75	2.62	2.71
Minimum-Maximum Density (g/cm ³)	ASTM D4253-16	1.1509-1.3706	1.658 - 1.937	1.445-1.696	1.6218-1.945
Minimum-Maximum Void Ratio	ASTM D4253-16	0.9699-1.3459	0.4249-0.6646	0.5448-0.8131	0.3676-0.6401
Fine Contents	ASTM D422	1.08%	11.63%	9.69%	4.19%
D ₁₀ (mm)	ASTM D 2487-06	0.13	0.065	0.075	0.15
D ₃₀ (mm)		0.18	0.28	0.21	0.47
D ₆₀ (mm)		0.24	0.85	0.35	1.6
C _u		1.84	13.08	4.67	10.67
C _c		1.04	1.42	1.68	0.92
Liquid Limit (%)	ASTM D4318-17	n/a	n/a	36	n/a
Plastic Limit (%)		n/a	n/a	27	n/a
Plasticity Index (%)		n/a	n/a	9	n/a
USCS Classification		SP (Poorly graded with little fines)	SW-SM (Well graded silty sand)	SP-SM (Poorly graded silty sand)	SW (Well Graded with little fines)

We can see from the results of the physical properties test stated in Table 4.1 that the Atterberg limits tests yielded results for only SER sand as it was the only sand that had enough cohesion to be moulded for the experiments. Even though GÜR sand had more fines than SER, the particles were cohesionless and unsuitable for the Atterberg limits tests.

4.2 Direct Shear Test (DST)

The DST was conducted on each of the four soil samples under normal loading of 27.8 kPa, 55.6 kPa and 83.3 kPa. These three runs result in an angle of friction for each sample tested under different water contents; 0%, 5% and 10%. The cohesion is indicated by an intercept of the angle of friction with the shear stress. The cohesion of sand is usually $c'=0$

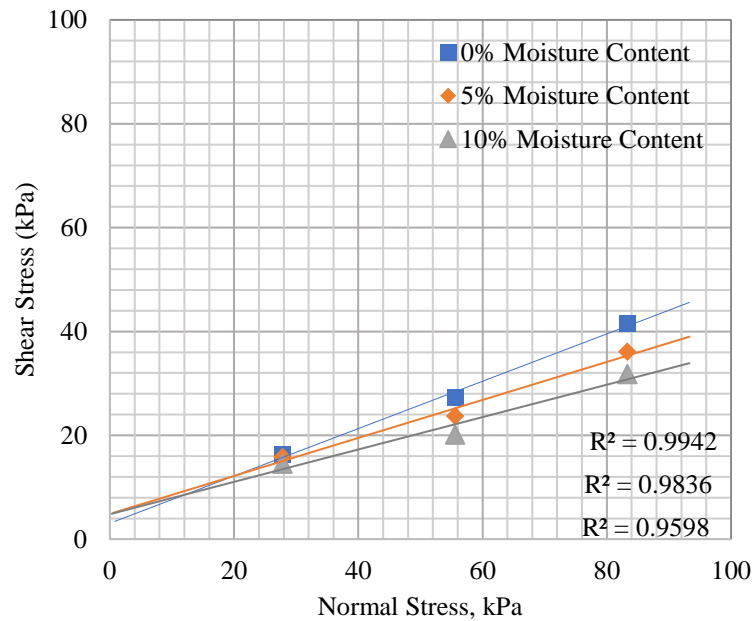


Figure 4.2: Normal Stress vs Shear Stress for GAZ

The shear strength of GAZ appears to be highest when the sample is dry, but decreases as the sample is tested at 5% and 10% water contents as seen in Figure 4.2. The same applies for the angle of friction, which also decreases as the water content of the tested sample was increased. The angle of friction values for 0%, 5% and 10% are 23° , 19.9° and 14.5° respectively. The cohesion however, increases as the sample is tested under increased water content. The respective cohesion values of the soil at 0%, 5% and 10% water contents are 3.1 kPa, 4.2 kPa and 6.3 kPa.

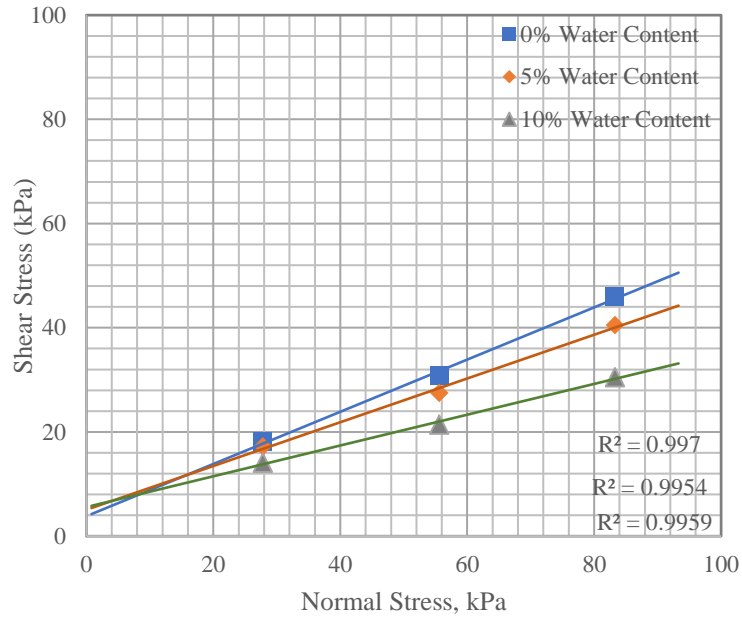


Figure 4.3: Normal Stress vs Shear Stress for GÜR

In Figure 4.3, we can see that GÜR sample shows the results expected in the DST, with the shear strength of the dry sample being the highest while showing the lowest cohesion value. The shear strength decreases when the water content of the samples increases (5% and 10%). The cohesion shows increase in value when the water content is increased. The cohesion values for 0%, 5% and 10% water contents are 4.8 kPa, 5.3 kPa and 5.7 kPa respectively. The angle of friction decreases, with respective values of 26°, 24°, and 17°.

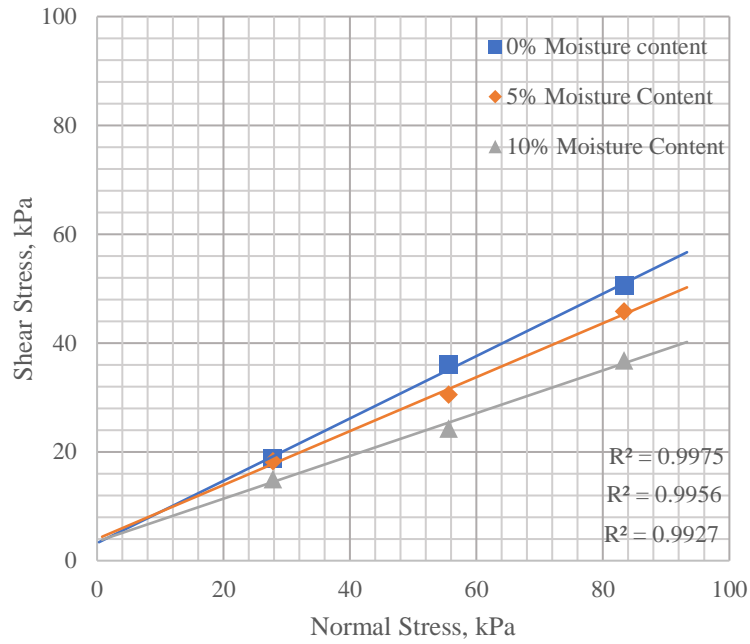


Figure 4.4: Normal Stress vs Shear Stress for SER

The shear stress of SER sample increased as the normal stress increased as seen in Figure 4.4. Samples with more water contents (5% and 10%) showed lower angles of but showed increased cohesion as illustrated in Figure 4.5. The dry sample had cohesion of 5.7 kPa and angle of friction of 28°, the sample with 5% Water content had cohesion of 5.8 kPa and angle of friction of 23°, while the 10% Water content had 6 kPa cohesion and angle of friction of 17°.

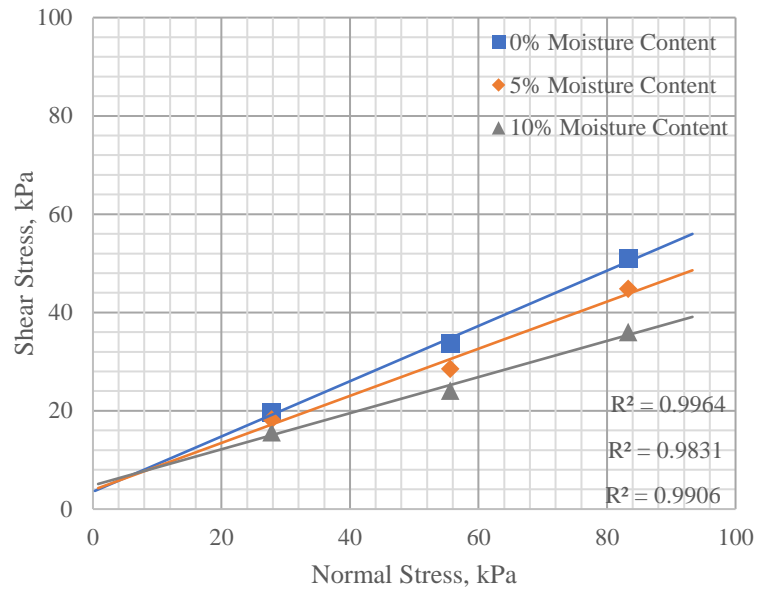


Figure 4.5: Normal Stress vs Shear Stress for RDQ

In Figure 4.5, the sample shows to have the highest shear strength with 0% water content, but drops as the water content increases to 5% and then 10%. The angle of friction also decreases as the water content increases. The angles of friction are 29°, 26° and 20.8° for 0%, 5% and 10% respectively.

Table 4.2: Comparison of shear strength parameter values of all four samples under the three water contents, 0%, 5% and 10%.

Sample	W (%)	Φ' (°)	c' (kPa)	R ²
GAZ	0%	23	3.1	0.9942
	5%	19.9	4.2	0.9836
	10%	14.5	5.2	0.9598
GÜR	0%	26	4.8	0.997
	5%	24	5.3	0.9954
	10%	17	5.7	0.9959
SER	0%	28	5.7	0.9975
	5%	23	5.8	0.9956
	10%	17	6	0.9927
RDQ	0%	29	2.8	0.9964
	5%	26	4	0.9831
	10%	20.8	5.3	0.9906

The normal stress-shear stress plot line all show a linearly increasing trend. The R² values in Table 4.2 prove that. The effective cohesion of sands is zero, although some sands can show some cohesion (Farouk et al., 2004).

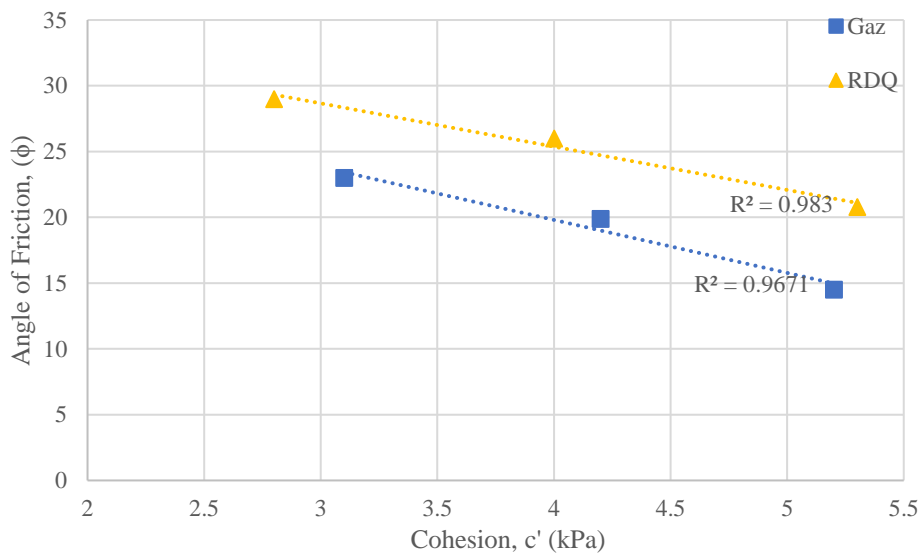


Figure 4.6: Comparison between cohesion and angle of friction for GAZ and RDQ samples

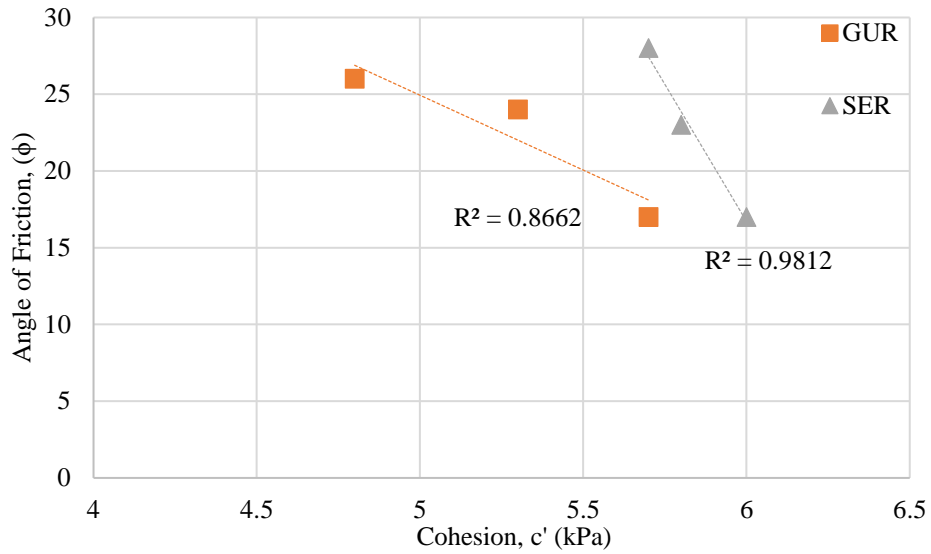


Figure 4.7: Comparison between cohesion and angle of friction for SER and GÜR samples

Figures 4.6 and 4.7 shows us that angle of friction decreases as the cohesion increases for all samples. The two samples with highest fine percentage (SER and GÜR) showed to have a sharper drop in angle of friction as the cohesion increases. This also coincides with having higher water content.

4.3 -Soil-Water Characteristics Curve (SWCC)

SWCC shows comparison between the matric suction and water content of the soil after undergoing wetting and drying suction procedures of the Tube Suction Test (TST). The TST provides a maximum matric suction of 100 kPa, a range that has been suitably used to conduct matric suction test on sands (Hong et al., 2016; Song, 2014; Song et al, 2012).

SWCC shows comparison between the matric suction and water content of the soil after undergoing wetting and drying suction procedures. The average water content is higher in the drying procedure than the wetting procedure due to the ink bottle effect (Song, 2014).

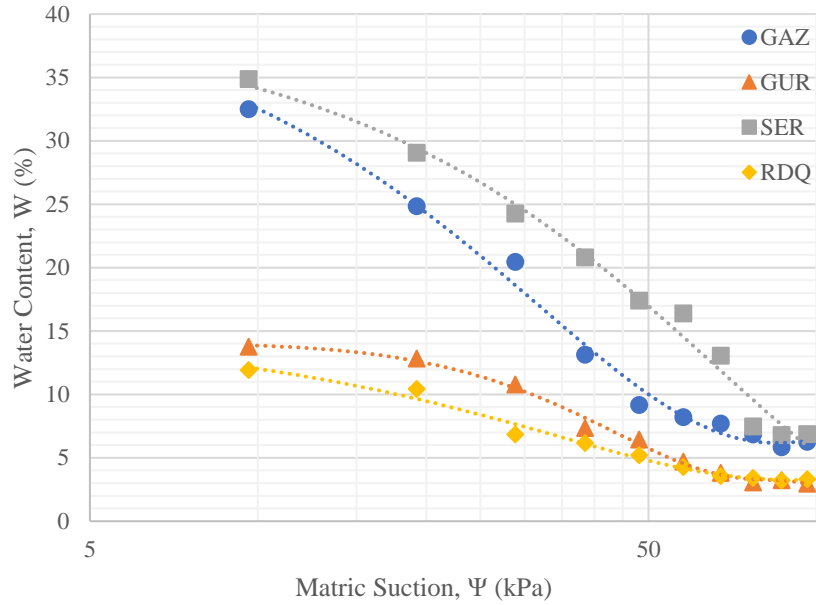


Figure 4.8: The SWCC for drying suction procedure comparing the resulting water contents of all four samples

From Figure 4.8, we can see that the sample that absorbed the most water was SER with 34.87%, followed by GAZ with 32.5%, GÜR with 13.75%, and the sample to absorb the least water was RDQ with 11.90%

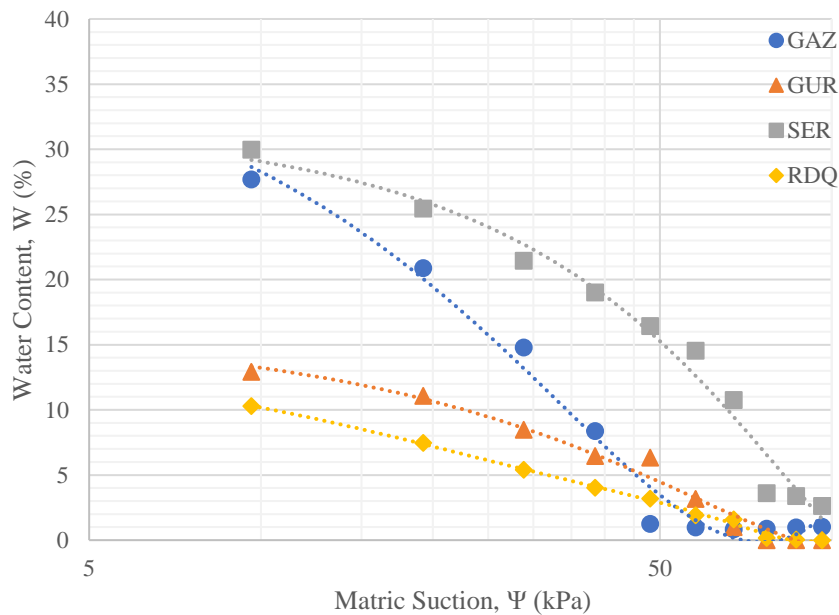


Figure 4.9: The SWCC for wetting suction procedure comparing the resulting water contents of all four samples.

The water content of each sand sample is at its highest when the matric suction is at its lowest as seen in Figure 4.9. The water content decreases as the matric suction increases. The sample that recorded the highest water is the Serhatkoy (SER) sample, absorbing as high as 29.97%. It is followed by GÜR with 27.68%, then SER with 12.92% and finally RDQ with 10.28%.

For all samples, the matric suction along the tube is at its lowest at the bottom of the tube and highest at the top. The TST provides a maximum matric suction of 100 kPa. The water content in the soil decreases with increasing suction, this also means it decreases as it goes up the tube. Figure 4.8 shows us the sample that absorbed the most water was SER with 34.87%, followed by GAZ with 32.5%, GÜR with 16.75%, and the sample to absorb the least water was RDQ with 11.90%. The two high absorbing samples, SER and GAZ, showed different characteristics as the water content decreased, with the latter showing a more dramatic decrease. The two crushed limestone sands appear to have the lowest capability of absorbing water as seen in Figure 4.8 and Figure 4.9.

The matric suction data for the samples were also placed through Fredlund and Xing (1994) (1994) and van Genuchten (1980) fits to test their suitability for SWCC. Each fit is based on its own equation used to predict the behaviour of SWCC for the samples. The water content and matric suction obtained from the laboratory are used in the equations. With the two fits, you can each estimate the Residual Water Content (RWC) and Air Entry Value (AEV) of each sample for wetting and drying processes. The SoilVision software was used to predict the fits for the SWCC diagrams for all samples.

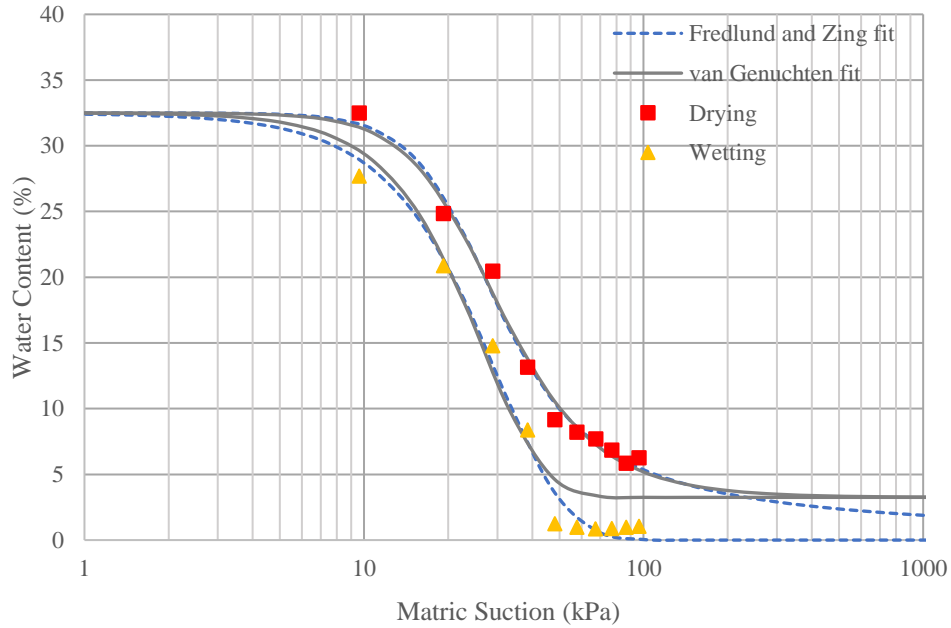


Figure 4.10: Fredlund and Xing (1994) and van Genuchten (1980) fits for both drying and wetting processes for GAZ

As expected, GAZ shows to have absorbed more water during drying process than during wetting process as seen in Figure. 4.10.

Table 4.3: Comparison of RWC and AEV of both Fredlund and Xing (1994) and van Genuchten (1980) fit for GAZ

Process	Fit	R ²	RWC (%)	AEV (kPa)
Drying	Fredlund and Xing	0.99	3.0	14.6
	van Genuchten	0.99	3.5	13.66
Wetting	Fredlund and Xing	0.99	0.0	11.68
	van Genuchten	0.94	3.5	11.68

For the drying process, both Fredlund and Xing (1994) and van Genuchten (1980) models show good fit for predicting the SWCC. Both models have R² values of 0.99 as seen in Table 4.3. The residual water content (RWC) values are 3.0% and 3.5% for respectively. The air entry values (AEV) are 14.6 kPa and 13.66 kPa respectively. The AEV for both models are close in value. For the wetting process, the R² value for the Fredlund and Xing (1994) model is 0.99, while for van Genuchten (1980) model, it is 0.94. Both models showing satisfactory

fits. The respective RWC values for both models are 0.0% and 3.5%. The AEVs are both 11.68 kPa. In both drying and wetting process, the Fredlund and Xing (1994) and van Genuchten (1980) models prove to be suitable for suction analysis of GAZ sand.

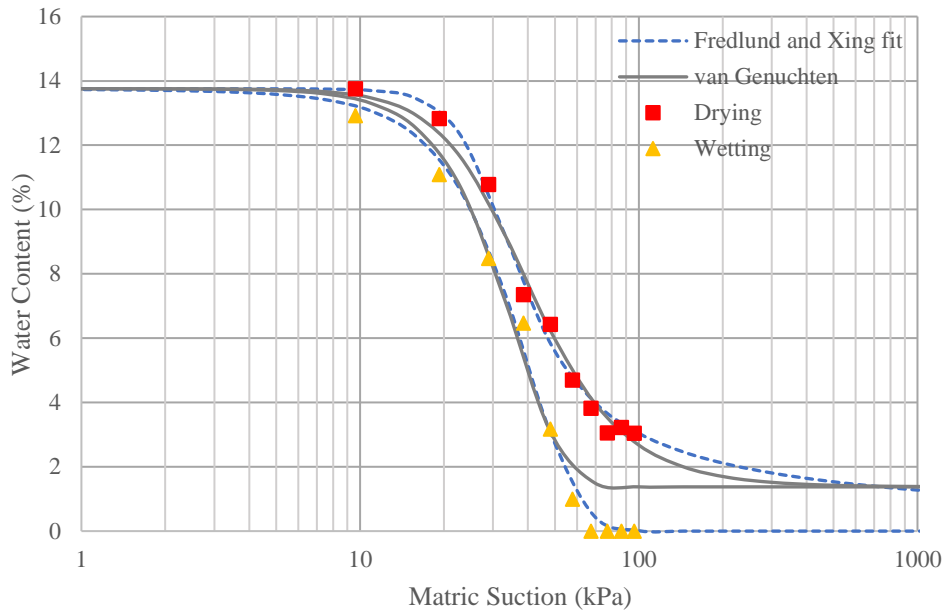


Figure 4.11: Fredlund and Xing (1994) and van Genuchten (1980) fits for both drying and wetting processes for GÜR

Table 4.4: Comparison of RWC and AEV of both Fredlund and Xing (1994) and van Genuchten (1980) fit for GÜR

Process	Fit	R ²	RWC	AEV
Drying	Fredlund and Xing	0.99	3.4	20
	van Genuchten	0.98	1.6	18.5
Wetting	Fredlund and Xing	0.99	0.0	18.5
	van Genuchten	0.95	1.6	18.5

For the drying process, the Fredlund and Xing (1994) and van Genuchten (1980) models fit well on the SWCC plot (shown in Figure 4.11), with R² values of 0.99 and 0.98 respectively (refer to Table 4.4). The RWC values are 3.4% and 1.6% respectively. The AEV are 20.0 kPa and 18.5 kPa respectively. For wetting process, the models also fit on the SWCC with respective R² values of 0.99 and 0.95. RWC for both models are 0.0% and 1.6% respectively with the AEV values at 18.5 kPa both.

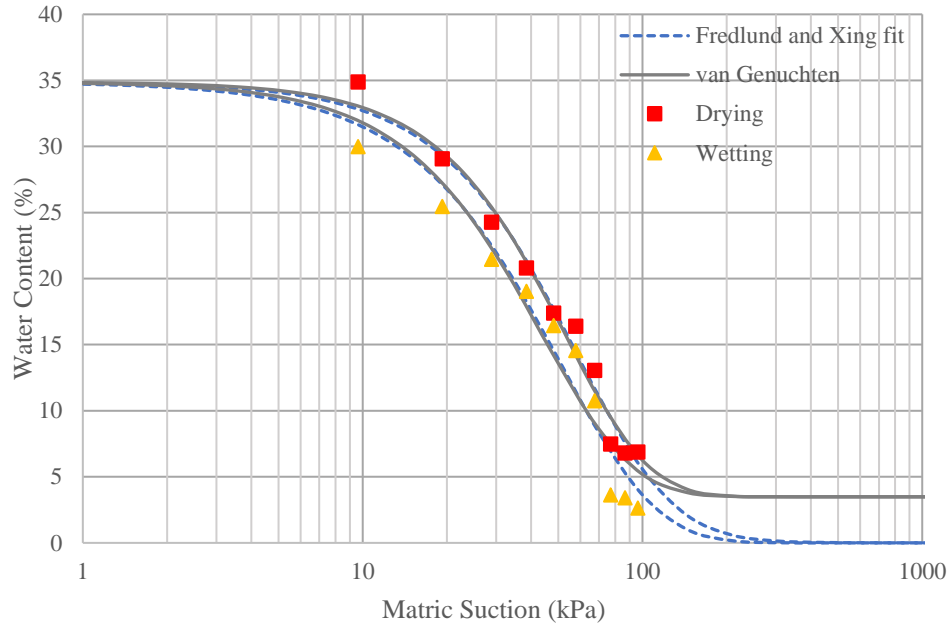


Figure 4.12: Fredlund and Xing (1994) and van Genuchten (1980) fits for both drying and wetting processes for SER

Table 4.5: Comparison of RWC and AEV of both Fredlund and Xing (1994) and van Genuchten (1980) fit for SER

Process	Fit	R ²	RWC	AEV
Drying	Fredlund and Xing	0.98	2.0	18.0
	van Genuchten	0.98	3.8	17.8
Wetting	Fredlund and Xing	0.95	2.0	14.5
	van Genuchten	0.98	3.8	14.5

The two prediction models that were applied fit the SWCC for the drying process (see Figure 4.12), showing R² values of 0.98 both (see Table 4.5). The RWC values for the two models are 2.0% and 3.8% respectively. The AEV are 18.0 kPa and 17.84 kPa respectively. For the wetting process, the SWCC prediction was a fit for both models, the R² values were 0.95 and 0.98 respectively (from Table 4.5). The wetting RWC were also 2.0% and 3.8% respectively for both models, while the respective AEV were 14.5 kPa both.

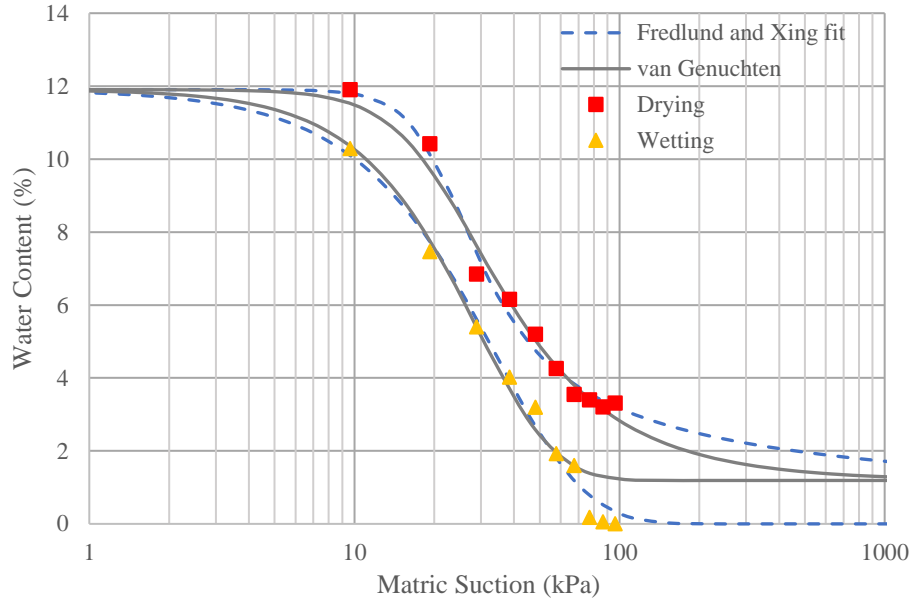


Figure 4.13: Fredlund and Xing (1994) and van Genuchten (1980) fits for both drying and wetting processes for RDQ

Table 4.6: Comparison of RWC and AEV of both Fredlund and Xing (1994) and van Genuchten (1980) fit for RDQ

Process	Fit	R ²	RWC	AEV
Drying	Fredlund and Xing	0.97	2.1	15.6
	van Genuchten	0.93	1.6	14.1
Wetting	Fredlund and Xing	0.99	0.0	9.6
	van Genuchten	0.99	1.2	9.3

Figure 4.13 shows us that the two models fit with the laboratory data. The Fredlund and Xing (1994) fit for the drying process recorded a RWC value of 2.1%, while the van Genuchten (1980) fit recorded 1.6%. The AEV were 15.6 kPa and 14.1 kPa respectively. As for the wetting process, the RWC values were also 0.0% and 1.2% respectively. The respective AEV were 9.6 kPa and 9.3 kPa (see Table 4.6).

Even after applying the prediction models, all samples show the hysteresis expected in SWCC. The drying process absorbed more water than the wetting process. The highest AEV value recorded was by GÜR with 20.00 kPa, followed by SER with 18.00 kPa, while GAZ and RDQ were close with 15.6 and 15.5 respectively. This order shows the effect that fine

percentage on the AEV; the higher the fine percentage, the higher the AEV value. The highest RWC value belonged to SER at 3.8%, followed by GAZ at 2.5%, then RDQ at 2.1%, with GÜR recording the lowest value of 1.6%. The RWC shows to be directly proportional to the moisture content absorbed during suction.

4.4 Matric Suction and Shear Strength

The relationship between shear strength and matric suction is analysed under the three normal stresses used in the direct shear test (DST), 27.8 kPa, 55.6 kPa and 83.3 kPa. The shear strength values were obtained using $\tau=c'+\sigma \tan\phi$. The matric suction was calculated using the capillary rise formula, matric suction= ρ_wgh . The shear strength increases as the matric suction increases in all normal stress cases, also implying the shear strength increases as the water content decreases. The shear strength records higher values as the normal stress is increased.

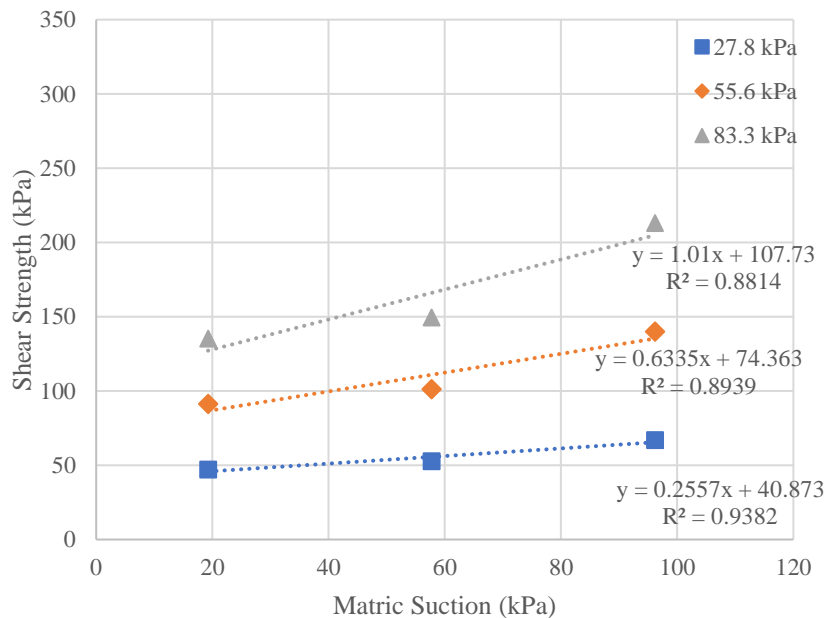


Figure 4.14: Matric Suction vs Shear Strength for GAZ under the three normal stresses

Figure 4.14 shows that, under the three normal stresses, 27.8 kPa, 55.6 kPa and 83.3 kPa, the shear strength increased as the matric suction increased. GAZ recorded its highest shear strength of 213.12 kPa.

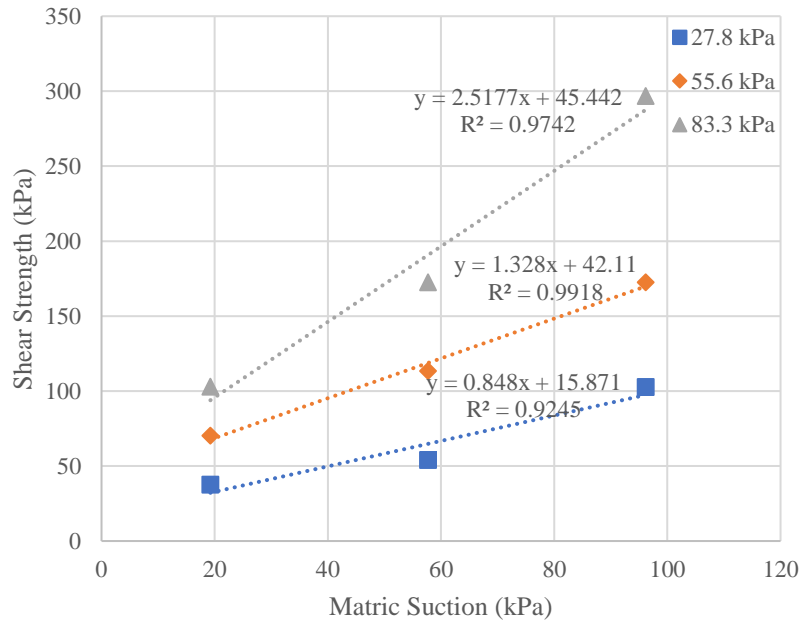


Figure 4.15: Matric Suction vs Shear Strength for GÜR under the three normal stresses

The shear strength shows to increase as the matric suction increases across the three normal stresses used in the DST, 27.8 kPa, 55.6 kPa and 83.3 kPa. This implies that the strength is lowest when the water content is at its highest. The sample shows the highest shear strength value of all four samples (compared in Table 4.7), as high as 296.74 kPa as seen in Figure 4.15.

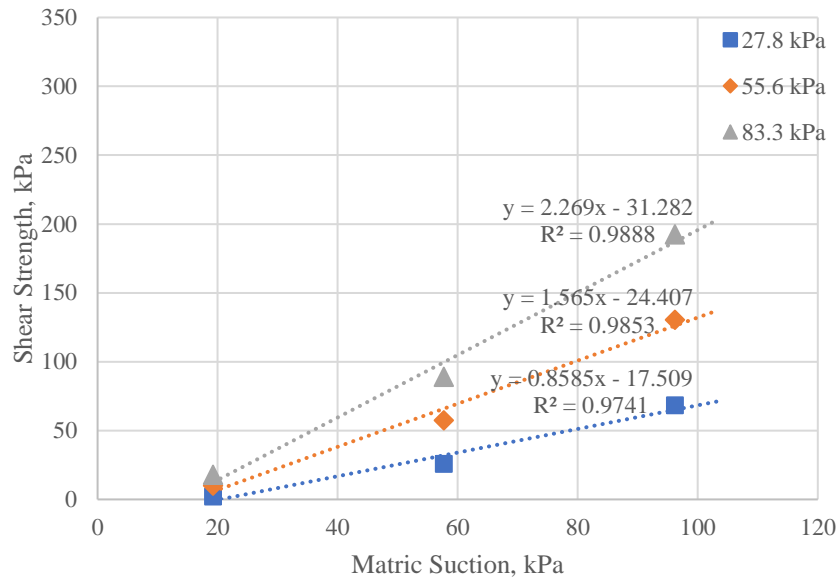


Figure 4.16: Matric Suction vs Shear Strength for SER under 19.2 kPa, 57.7 kPa and 96.2 kPa normal stresses

The shear strength of SER shows an increase when the matric suction in the soil increases. The sample showed lower shear strength at lower matric suction. This means the shear strength is lower with higher water content. The highest strength showed by the sample is 192.36 kPa (see Figure 4.16). The sample showed to have the lowest shear strength of all four samples (stated in Table 4.7).

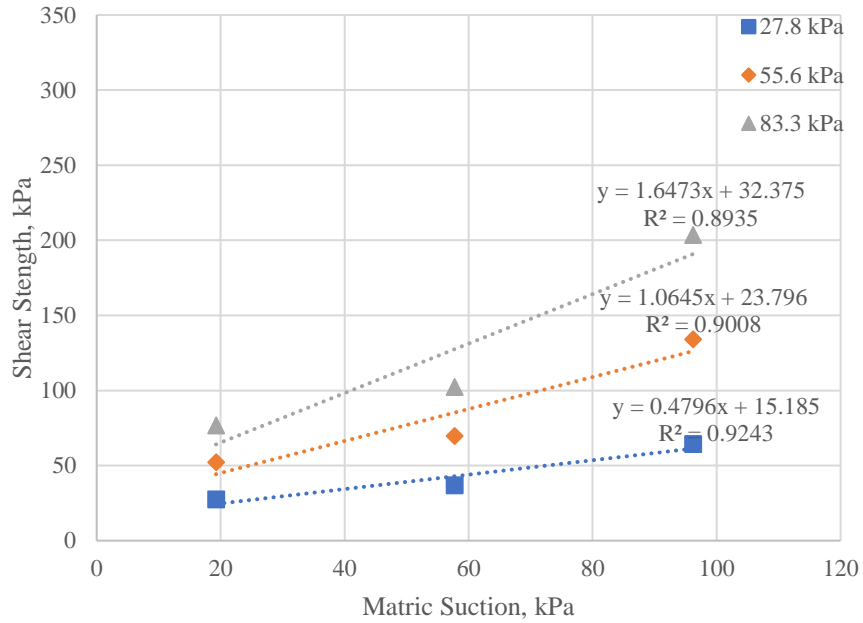


Figure 4.17: Matric Suction vs Shear Strength for RDQ under 19.2 kPa, 57.7 kPa and 96.2 kPa normal stresses

In Figure 4.17, we can see RDQ sand shows the same pattern as the other sands, as the shear strength increased across all normal stress with increasing matric suction. The highest shear strength RDQ recorded is 203.47 kPa.

Table 4.7: Comparison of shear strength and matric suction of all samples under three normal stresses

Sample	Suction (kPa)	Shear strength (kPa)		
		$\sigma'_1 = 27.8$ kPa	$\sigma'_2 = 55.6$ kPa	$\sigma'_3 = 83.3$ kPa
GAZ	19.23937	47.2507	91.4013	135.393
	57.71812	52.7141	101.228	149.568
	96.19686	66.9271	140.154	213.118
GÜR	19.23937	37.5693	70.3387	102.99
	57.71812	54.0501	113.4	172.537
	96.19686	102.831	172.537	296.743
SER	19.23937	2.12	9.95	17.7431
	57.71812	25.82	57.43	88.94
	96.19686	68.19	130.39	192.36
RDQ	19.23937	27.4626	52.1251	76.699
	57.71812	36.7693	69.5387	102.19
	96.19686	64.3734	134.047	203.47

The four samples showed the same linear increase in shear strength as the matric suction increased across all normal stresses. These results are summarised in Table 4.7.

Table 4.8: Comparison of line trends of matric suction versus shear strength according to the normal stresses

Sample	σ' (kPa)	R²
GAZ	27.8	0.9382
	55.6	0.8939
	83.3	0.8814
GÜR	27.8	0.9245
	55.6	0.9918
	83.3	0.9742
SER	27.8	0.9741
	55.6	0.9853
	83.3	0.9888
RDQ	27.8	0.9243
	55.6	0.9008
	83.3	0.8935

Table 4.8 shows us the line fit that indicates the linear increase in shear strength as the matric suction increases.

CHAPTER 5

CONCLUSION AND RECOMMENDATIONS

5.1 Conclusion

The tube suction test has been found to be a successful way of measuring the suction ability of various sands that can be found in North Cyprus, even though it is not a standard test method. The method can calculate suction as high as 100 kPa.

GAZ and the two crushed limestone sands (GÜR and RDQ) did not have much cohesion to be applied successfully in the Atterberg limit test. But the yellow sand (SER) was cohesive enough to be moulded for the tests.

Sands are considered to have zero effective cohesion, but they may show some level of cohesion in the shear test results. SER and GÜR had the highest fine content, 9.69% and 11.63% respectively, and showed some cohesion. SER in particular showed significant cohesion possibly because of its mineralogy. Increase in cohesion has a negative effect on angle of friction, making it to decrease. Samples with higher fine percentage have shown a steeper decrease in angle of friction. The increase in water content means increase in cohesion. It implies that the higher the matric suction, the lower the cohesion the sand may have. This is because the sand contains less water at higher suction range.

The two poorly graded sands (GAZ and SER) absorbed the highest amount of water at the lowest levels of matric suction. SER absorbed the highest water content (34.87%). The water content of GAZ sand however, dropped drastically as the matric suction increased compared to that of SER. The two crushed limestone sands (GÜR and RDQ) are well graded and absorbed less water than the other two sands. RDQ had the lowest water content of 11.90%.

The Fredlund and Xing (1994) and van Genuchten (1980) models have proven to be successful for predicting SWCC of all four sands. They also show the same hysteresis as the manual data; with the drying curve being higher than the wetting curve. The air entry value (AEV) and residual water content (RWC) were successfully determined using both models. The AEV and RWC gave similar values from both drying and wetting curves for all samples. The soil parameters used in the two models were successfully obtained from the SoilVision software.

The shear strength showed to be directly proportional to the matric suction; meaning it increases as the matric suction increases.

The fine percentage showed to affect the air entry value (AEV) directly. The sands with the highest fine percentage had higher AEV. Meanwhile, the RWC values showed to be affected by the water content absorbed during suction. The higher the water content, the higher the RWC.

5.2 Recommendations

1. The effects of adding different types of soils such as clay or gravel to the samples could be investigated for any changes in suction and shear strengths characteristics.
2. Crushed sands from other types of rocks can also be investigated for suction and shear strength characteristics. Differences in mineralogy could also be investigated.
3. Changes could be made to modify the particle size distribution of the samples in order to give certain suction and shear strength characteristics which may be suitable for certain purposes.
4. Shear strength test could be performed under more number of water content and with other shear strength testing methods.

5. The tubes used in this tube suction test could be modified to read water content without the need for removal of sample. This could be done with the help of a percometer.

REFERENCES

- Adunoye, G. O. (2014). Study of Relationship between Fines Content and Cohesion of Soil, *4*(4), 682–692.
- Agus, S. S., & Schanz, T. (2005). Comparison of Four Methods for Measuring Total Suction. *Vadose Zone Journal*, *4*(4), 1087. <https://doi.org/10.2136/vzj2004.0133>
- Al-Khafaf, S., & Hanks, R. J. (1974). Evaluation of The Filter Paper Method For Estimating Soil Water Potential. Retrieved December 24, 2017, from http://journals.lww.com/soilsci/Abstract/1974/04000/Evaluation_of_the_Filter_Paper_Method_for.3.aspx
- Aldaood, A., Bouasker, M., & Al-Mukhtar, M. (2014). Soil–water characteristic curve of lime treated gypseous soil. *Applied Clay Science*, *102*, 128–138. <https://doi.org/10.1016/J.CLAY.2014.09.024>
- Alias, R., Kasa, A., & Taha, M. R. (2014). Particle size effect on shear strength of granular materials in direct shear test. *International Journal of Civil, Structural, Construction and Architectural Engineering*, *8*(11), 733–736.
- Barrett, E., & Beskeen, L. (1986). *Resource Book: Let's Look at Sand*. Mineral Industry Manpower and Careers Unit.
- Benson, C., & Bosscher, P. (1999). Time-domain Reflectometry (TDR) in Geotechnics: A Review. In *Nondestructive and Automated Testing for Soil and Rock Properties* (pp. 113-113–24). 100 Barr Harbor Drive, PO Box C700, West Conshohocken, PA 19428-2959: ASTM International. <https://doi.org/10.1520/STP13313S>
- Bulut, R., Lytton, R. L., & Wray, W. K. (2001). Soil suction measurements by filter paper.

- Expansive Clay Soils and Vegetative Influence on Shallow Foundations*, 243–261.
[https://doi.org/10.1061/40592\(270\)14](https://doi.org/10.1061/40592(270)14)
- Choi, Y., & Choi, J. (2013). A Comparative Study of Concretes Containing Crushed Limestone Sand and Natural Sand. *Open Journal of Civil Engineering*, 2013(3), 13–18.
- Çokça, E., & Tilgen, H. P. (2010). Shear strength-suction relationship of compacted Ankara clay. *Applied Clay Science*, 49(4), 400–404. <https://doi.org/10.1016/j.clay.2009.08.028>
- Dafalla, M. A. (2013). Effects of clay and moisture content on direct shear tests for clay-sand mixtures. *Advances in Materials Science and Engineering*, 2013. <https://doi.org/10.1155/2013/562726>
- Das, B. M. (2008). *Geotechnical Engineering* (Vol. 53). Global Publishing Program. <https://doi.org/10.1017/CBO9781107415324.004>
- Delage, P. (2008). Experimental unsaturated soil mechanics, 1961(3), 973–996. <https://doi.org/10.2136/vzj2009.0115br>
- Elgabu, H. M. (2013). Critical evaluation of some suction measurement techniques, 268.
- Farouk, A., Lamboj, L., & Kos, J. (2004). Influence of matric suction on the shear strength behaviour of unsaturated sand. *Acta Polytechnica*, 44(4), 11–17. Retrieved from <https://ojs.cvut.cz/ojs/index.php/ap/article/view/590>
- Fredlund, D. G., & Houston, S. L. (2013). Interpretation of soil-water characteristic curves when volume change occurs as soil suction is changed. *Advances in Unsaturated Soils*, c, 15–31. <https://doi.org/doi:10.1201/b14393-410.1201/b14393-4>
- Fredlund, D. G., & Wong, D. K. H. (1989). Calibration of thermal conductivity sensors for

measuring soil suction. Retrieved from Fredlund, Wong - 1989 - Calibration of thermal conductivity sensors for measuring soil suction.pdf

Fu, W., Zheng, X., Lei, X., & Deng, J. (2015). Using a modified direct shear apparatus to explore gap and size effects on shear resistance of coarse-grained soil. *Particuology*, 23, 82–89. <https://doi.org/10.1016/j.partic.2014.11.013>

Gao, Y., & Sun, D. (2017). Soil-water retention behavior of compacted soil with different densities over a wide suction range and its prediction. *Computers and Geotechnics*, 91, 17–26. <https://doi.org/10.1016/J.COMPGeo.2017.06.016>

Ghanbarian-Alavijeh, B., Liaghat, A., Huang, G. H., & Van Genuchten, M. T. (2010). Estimation of the van Genuchten Soil Water Retention Properties from Soil Textural Data. *Pedosphere*, 20(4), 456–465. [https://doi.org/10.1016/S1002-0160\(10\)60035-5](https://doi.org/10.1016/S1002-0160(10)60035-5)

Heinrich, E. W. (2001). Economic Geology of The Sand and Sandstone Resources of Michigan Survey Division Report of Investigation 21. Retrieved from http://www.michigan.gov/documents/deq/GIMDL-RI21_216264_7.pdf

Hong, W. T., Jung, Y. S., Kang, S., & Lee, J. S. (2016). Estimation of soil-water characteristic curves in multiple-cycles using membrane and TDR system. *Materials*, 9(12). <https://doi.org/10.3390/ma9121019>

Houlsby, G. T. (1991). How the dilatancy of soils affects their behaviour. *Proceedings of the 10th European Conference on Soil Mechanics and Foundation Engineering*. Retrieved from http://www.eng.ox.ac.uk/civil/publications/reports-1/ouel_1888_91.pdf

Kassem, E., Masad, E., Lytton, R., & Bulut, R. (2009). Measurements of the moisture diffusion coefficient of asphalt mixtures and its relationship to mixture composition. *International Journal of Pavement Engineering*, 10(6), 389–399.

<https://doi.org/10.1080/10298430802524792>

- Kim, J. K., Lee, C. S., Park, C. K., & Eo, S. H. (1997). The fracture characteristics of crushed limestone sand concrete. *Cement and Concrete Research*, 27(11), 1719–1729. [https://doi.org/10.1016/S0008-8846\(97\)00156-7](https://doi.org/10.1016/S0008-8846(97)00156-7)
- Konyai, S., Sriboonlue, V., & Trelo-Ges, V. (2009). The effect of air entry values on hysteresis of water retention curve in saline soil. *American Journal of Environmental Sciences*, 5(3), 341–345. <https://doi.org/10.3844/ajessp.2009.341.345>
- Krahn, J., & Fredlund, D. G. (1972). on Total, Matric and Osmotic Suction. *Soil Science*. <https://doi.org/10.1097/00010694-197211000-00003>
- Kurucuk, N., Kodikara, J., & Fredlund, D. G. (2012). *Null-type axis-translation technique: Is it applicable to soils with low saturation? 5th Asia-Pacific Conference on Unsaturated Soils 2012* (Vol. 1).
- Kyonka, J. C., & Cook, R. L. (1954). The Properties of Feldspars and Their Use in Whitewares. *University of Illinois Bulletin*, 1–34.
- Lambe, T. W. (1982). *Soil testing for engineers*. Wiley.
- Lee, R., & Fredlund, D. (1984). Measurement of Soil Suction Using the MCS 6000 Gauge..pdf. *Fifth International Conference on Expansive Soils 1984: Preprints of Papers*.
- Leong, E.-C., Tripathy, S., & Rahardjo, H. (2003). Total suction measurement of unsaturated soils with a device using the chilled-mirror dew-point technique. *Géotechnique*, 53(2), 173–182. <https://doi.org/10.1680/geot.2003.53.2.173>

- Lourenço, S. D. N., Gallipoli, D., Toll, D. G., & Evans, F. D. (2006). Development of a Commercial Tensiometer for Triaxial Testing of Unsaturated Soils. In *Unsaturated Soils 2006* (pp. 1875–1886). Reston, VA: American Society of Civil Engineers. [https://doi.org/10.1061/40802\(189\)158](https://doi.org/10.1061/40802(189)158)
- Marjerison, B., Richardson, N., Widger, A., Fredlund, D. G., & Berthelot, C. (2001). Installation of sensors and measurement of soil suction below thin membrane surface pavements in Saskatchewan.
- Meissner, T. (2004). Relationship between soil properties of Mallee soils and parameters of two moisture characteristics models. *SuperSoil 2004 - 3rd Australian New Zealand Soils Conference, University of Sydney, Australia*, (December), 1–10.
- Menadi, B., Kenai, S., Khatib, J., & Ait-Mokhtar, A. (2009). Strength and durability of concrete incorporating crushed limestone sand. *Construction and Building Materials*, 23(2), 625–633. <https://doi.org/10.1016/j.conbuildmat.2008.02.005>
- Nichol, C., Smith, L., & Beckie, R. (2003). Long-term measurement of matric suction using thermal conductivity sensors. *Canadian Geotechnical Journal*, 40(3), 587–597. <https://doi.org/10.1139/t03-012>
- Pan, H., Qing, Y., & Pei-yong, L. (2010). Direct and indirect measurement of soil suction in the laboratory. *Electronic Journal of Geotechnical Engineering (EJGE)*, 15, 1–13. Retrieved from <http://ejge.com/2010/Ppr10.009/Ppr10.009.pdf>
- Pinard, M. I., Paige-Green, P., Mukura, K., & Motswagole, K. J. (2013). Guideline on the Use of Sand in Road Construction in the SADC Region, (May).
- Richards, B. G. (1965). Measurement of the free energy of soil moisture by the psychrometric technique using thermistors. Sydney, N.S.W., Butterworths. Retrieved from <https://publications.csiro.au/rpr/pub?list=BRO&pid=procite:132e4d9c-bfde->

4a87-a3e2-d513f88a6b76

- Ridley, A. M., & Wray, W. K. (1996). Suction Measurement: A Review of Current Theory and Practices (p. 1573). Presses de l'École nationale des ponts et chaussées. Retrieved from <https://trid.trb.org/view/575095>
- Sawicki, A. (2014). Dilation and modelling of sands in the light of experimental data. *Archives of Hydroengineering and Environmental Mechanics*, 61(1–2), 3–15. <https://doi.org/10.1515/heem-2015-0001>
- Shakkour, O., Rabb, I., & Sadeq, A. (2015). Feldspar. Retrieved from <http://www.memr.gov.jo/EchoBusV3.0/SystemAssets/PDFs/AR/MineralTR/Feldspar.pdf>
- Shaw, B., & Baver, L. D. (1939). An Electrothermal Method for Following Moisture Changes of the Soil in Situ. *Soil Science Society of America Journal*, 4(C), 78. <https://doi.org/10.2136/sssaj1940.036159950004000C0014x>
- Sheng, D., Gens, A., Fredlund, D. G., & Sloan, S. W. (2008). Unsaturated soils: From constitutive modelling to numerical algorithms. *Computers and Geotechnics*, 35(6), 810–824. <https://doi.org/10.1016/j.compgeo.2008.08.011>
- Song, Y. S. (2014). Suction stress in unsaturated sand at different relative densities. *Engineering Geology*, 176, 1–10. <https://doi.org/10.1016/j.enggeo.2014.04.002>
- Southard, J. (2007). Chapter 4 Siliclastic Rocks. *Sedimentary Geology*, 92–116.
- Spanner, D. C. (1951). The Peltier Effect and its Use in the Measurement of Suction Pressure. *Journal of Experimental Botany*, 2(2), 145–168. <https://doi.org/10.1093/jxb/2.2.145>

- Tang, G. X., Graham, J., Blatz, J., Gray, M., & Rajapakse, R. K. N. D. (2002). Suctions, stresses and strengths in unsaturated sand-bentonite. *Engineering Geology*, *64*(2–3), 147–156. [https://doi.org/10.1016/S0013-7952\(01\)00108-9](https://doi.org/10.1016/S0013-7952(01)00108-9)
- Toker, N. K. (2002). *Improvements and reliability of MIT tensiometers and studies on soil moisture characteristic curves*. Retrieved from <http://dspace.mit.edu/handle/1721.1/26891>
- Topp, G. C., Davis, J. L., & Annan, A. P. (1980). Electromagnetic determination of soil water content: Measurements in coaxial transmission lines. *Water Resources Research*, *16*(3), 574–582. <https://doi.org/10.1029/WR016i003p00574>
- Vanapalli, S. K., Fredlund, D. G., & Pufahl, D. E. (1996). The relationship between the soil-water characteristic curve and the unsaturated shear strength of a compacted glacial till. *Geotechnical Testing Journal*, *19*(3), 259–268. <https://doi.org/10.1520/GTJ10351J>
- Wiederhold, P. R. (1997). *Water vapor measurement*. Marcel Dekker. Retrieved from <https://www.crcpress.com/Water-Vapor-Measurement-Methods-and-Instrumentation/Wiederhold/p/book/9780824793197>
- Woodburn, J. A., Holden, J. C., & Peter, P. (1993). The Transistor Psychrometer: A New Instrument for Measuring Soil Suction. ASCE. Retrieved from <http://cedb.asce.org/CEDBsearch/record.jsp?dockey=0085324>
- Yang, H., Rahardjo, H., Leong, E. C., & Fredlund, D. G. (2004). A study of infiltration on three sand capillary barriers. *Canadian Geotechnical Journal*, *41*(4), 629–643. <https://doi.org/10.1139/t04-021>
- Yang, X., & You, X. (2013). Estimating parameters of van genuchten model for soil water retention curve by intelligent algorithms. *Applied Mathematics and Information Sciences*, *7*(5), 1977–1983. <https://doi.org/10.12785/amis/070537>

- Yu, X., & Drnevich, V. P. (2004). Soil water content and dry density by time domain reflectometry. *Journal of Geotechnical and Geoenvironmental Engineering*, 130(9), 922–934. [https://doi.org/10.1061/\(ASCE\)1090-0241\(2004\)](https://doi.org/10.1061/(ASCE)1090-0241(2004))
- Zhai, Q., Rahardjo, H., & Satyanaga, A. (2017). Effects of residual suction and residual water content on the estimation of permeability function. *Geoderma*, 303, 165–177. <https://doi.org/10.1016/J.GEODERMA.2017.05.019>
- Zhou, W. H., Xu, X., & Garg, A. (2016). Measurement of unsaturated shear strength parameters of silty sand and its correlation with unconfined compressive strength. *Measurement: Journal of the International Measurement Confederation*, 93, 351–358. <https://doi.org/10.1016/j.measurement.2016.07.049>
- Zoubir, M., Tayeb, B., Madani, B., & Mourad, H. (2014). Mix Proportioning And Performance Of A Crushed Limestone Sand-Concrete. *Journal of Building Materials and Structures*, 1(1), 10–22. <https://doi.org/10.5281/ZENODO.241875>